MOLECULAR AND CELLULAR BIOLOGY, July 1996, p. 3637–3650 Vol. 16, No. 7
0270-7306/96/$04.00+0

Signaling in the Yeast Pheromone Response Pathway: Specific and High-Affinity Interaction of the Mitogen-Activated Protein (MAP) Kinases Kss1 and Fus3 with the Upstream MAP Kinase Kinase Ste7

LEE BARDWELL,[1] JEANETTE G. COOK,[1] ERNIE C. CHANG,[1] BRADLEY R. CAIRNS,[2] AND JEREMY THORNER[1]*

Department of Molecular and Cell Biology, Division of Biochemistry and Molecular Biology, University of California, Berkeley, California 94720-3202,[1] and Department of Cell Biology, Stanford University School of Medicine, Stanford, California 94305[2]

Received 29 December 1995/Returned for modification 19 February 1996/Accepted 29 March 1996

Kss1 and Fus3 are mitogen-activated protein kinases (MAPKs or ERKs), and Ste7 is their activating MAPK/ERK kinase (MEK), in the pheromone response pathway of *Saccharomyces cerevisiae*. To investigate the potential role of specific interactions between these enzymes during signaling, their ability to associate with each other was examined both in solution and in vivo. When synthesized by in vitro translation, Kss1 and Fus3 could each form a tight complex (K_d of ~5 nM) with Ste7 in the absence of any additional yeast proteins. These complexes were specific because neither Hog1 nor Mpk1 (two other yeast MAPKs), nor mammalian Erk2, was able to associate detectably with Ste7. Neither the kinase catalytic core of Ste7 nor the phosphoacceptor regions of Ste7 and Kss1 were necessary for complex formation. Ste7-Kss1 (and Ste7-Fus3) complexes were present in yeast cell extracts and were undiminished in extracts prepared from a *ste5*Δ*ste11*Δ double mutant strain. In Ste7-Kss1 (or Ste7-Fus3) complexes isolated from naive or pheromone-treated cells, Ste7 phosphorylated Kss1 (or Fus3), and Kss1 (or Fus3) phosphorylated Ste7, in a pheromone-stimulated manner; dissociation of the high-affinity complex was shown to be required for either phosphorylation event. Deletions of Ste7 in the region required for its stable association with Kss1 and Fus3 in vitro significantly decreased (but did not eliminate) signaling in vivo. These findings suggest that the high-affinity and active site-independent binding observed in vitro facilitates signal transduction in vivo and suggest further that MEK-MAPK interactions may utilize a double-selection mechanism to ensure fidelity in signal transmission and to insulate one signaling pathway from another.

Cellular responses to external signals are elicited by sets of regulatory proteins that act in a cascade. The individual tiers of such cascades function first to transduce the extracellular stimulus across the plasma membrane and then to transmit, amplify, and disseminate the initial signal to multiple effectors. The pathway utilized by the yeast *Saccharomyces cerevisiae* to respond to the presence of its peptide mating pheromones is arguably the most thoroughly characterized multicomponent signaling network in any eukaryotic cell (for reviews, see references 5, 55, and 87). This pathway is activated when a pheromone that has been secreted by cells of one haploid mating type binds to a seven-transmembrane-segment receptor on a cell of the opposite mating type. Receptor occupancy causes activation of a coupled heterotrimeric G protein on the inner face of the plasma membrane (94). The signal is then transmitted by the βγ subunits of the G protein to a series of components including Cdc42, a member of the rho family of GTP-binding proteins (82, 97), Ste20, a protein kinase homologus to mammalian PAK (73, 95), and the multifunctional protein Ste5 (30, 40). The exact order of function of these proteins is not yet clear.

Next, the signal is transmitted to a protein kinase cascade composed of the Ste11, Ste7, Kss1, and Fus3 protein kinases. Ste11 phosphorylates and activates (66) the dual-specificity protein kinase, Ste7, which, in turn, phosphorylates and activates (14, 33, 88, 99) the Ser-, Thr-specific protein kinases, Fus3 (35) and Kss1 (59). The Ste11-Ste7-Kss1/Fus3 protein kinases comprise a so-called mitogen- or messenger-activated protein kinase (MAPK) cascade (for reviews, see references 2, 8, 41, and 57). MAPK cascades are found ubiquitously in eukaryotic organisms, in which they have been implicated in growth control, differentiation, tumorigenesis, and cellular stress responses (15, 19, 62). The *KSS1* (22), *STE7* (90), and *STE11* (76) genes were, respectively, the first MAPK (or ERK, for extracellular-signal-regulated kinase), MEK (for MAPK/ERK kinase), and MEKK (for MEK kinase) isolated from any organism. Fus3, like Kss1, is a member of the MAPK family (28); in pheromone response, these two enzymes are largely redundant in function (31, 59, 92).

Among the known or suspected downstream targets of Fus3 and Kss1 in the mating pathway are Ste12 (a transcriptional activator) (29, 84) and Far1 (a Cdk inhibitor specific for the G_1 cyclin-bound forms of the $p34^{CDC28}$ protein kinase) (69, 70). These two effectors are thought to be largely responsible for mediating two of the most obvious and most immediate physiological responses to pheromone, namely, enhanced transcription of a battery of pheromone-inducible genes and arrest of the cell division cycle in the late G_1 phase. These changes initiate a series of other events, which culminate in the conju-

* Corresponding author. Mailing address: Department of Molecular and Cell Biology, Division of Biochemistry and Molecular Biology, Room 401, Barker Hall, Corner of Hearst and Oxford St., Berkeley, CA 94720-3202. Phone: (510) 642-2558. Fax: (510) 643-5035. Electronic mail address: jthorner@mendel.berkeley.edu.

gation (mating) of two haploid cells of the opposite mating type.

The budding yeast *S. cerevisiae* contains at least three other discrete signaling cascades that lead to the activation of MAPKs (41, 57). Cells respond to high osmolarity by activating Hog1; proper cell wall synthesis requires a protein kinase C-dependent pathway that leads to activation of Mpk1/Slt2; and, during sporulation, Smk1 becomes activated. Moreover, a pathway necessary for haploid cells to manifest invasive growth utilizes Ste11, Ste7, and Kss1 (but not Fus3) and probably an as yet unidentified MAPK family member as well (77). Following their discovery in *S. cerevisiae*, parallel MAPK cascades were also found in mammalian cells (8, 16, 25). The mechanisms involved in the maintenance of specificity from stimulus to cellular response in the face of parallel MAPK cascades containing highly conserved (or, in some cases, even identical) components are largely unexplored.

In recent years, it has become widely appreciated that rather stable protein-protein interactions among components of intracellular signaling cascades exist and appear to play an important role in signal propagation (3, 7, 20). The roles of certain protein-protein interactions in signal transmission are relatively clear, but, in many cases, the complexity of protein-protein associations observed (30, 79) seems inconsistent with a simple model in which signal transduction proceeds down a strictly linear pathway, with successive steps serving to amplify the signal. Indeed, stable protein-protein interactions could serve to facilitate other aspects of signaling, including spreading an initial signal to two (or more) branches of a pathway (signal dissemination), regulating the amplitude and duration of a signal by feedback or feed-forward mechanisms (signal modulation), mediating appropriate cross talk between one pathway and another (signal integration), and avoiding inappropriate or adventitious activation or inhibition of one pathway by another (signal insulation). However, there has been little direct experimental support for such suggestions.

We describe here experiments that demonstrate a direct, specific, and relatively stable physical interaction between a MEK, Ste7, and each of its downstream MAPKs, Kss1 and Fus3. Moreover, we define some of the structural requirements for this high-affinity association and show other evidence indicating that the complex is most likely not a MEK-MAPK or a MAPK-MEK enzyme-substrate complex (ES complex). Furthermore, using additional biochemical and genetic approaches, we explore the role of this interaction in the efficient propagation of a signal in the pheromone response pathway in vivo.

MATERIALS AND METHODS

Yeast strains, culture conditions, genetic procedures, and recombinant DNA methods. Yeast strains used in this work are listed in Table 1. Media for yeast cell growth were prepared as described previously (80) except that in synthetic minimal media, twice the recommended level of amino acid supplements was used. Conventional methods were used for all recombinant DNA manipulations in bacteria (78). *Escherichia coli* DH5αF′ was used as the host for construction and propagation of all plasmids. DNA-mediated transformation of yeast cells was performed with lithium acetate-treated cells and single-stranded DNA as the carrier (36). To construct the *ste5*Δ *ste11*Δ strain, plasmid pSURE11 (40) was digested with *Bam*HI and *Xho*I, and the resulting 6.8-kb fragment (containing a *ste11*Δ::*hisG-URA3-hisG* allele) was used to transform a *ste5*Δ strain, SY1492. Ura^+ transformants were selected, and successful transplacement of the *STE11* locus was verified by acquisition of a sterile phenotype that was complementable by cotransformation with both a *STE11*-containing plasmid and a *STE5*-containing plasmid but not by either plasmid alone. One such isolate (YLB102) was plated on 5-fluoro-orotic acid medium (9) to select for a Ura^- derivative (YLB103), in which the *ste5*Δ *ste11*Δ phenotype was again verified.

Yeast expression vectors. To overexpress Ste7 or a fully functional derivative of Ste7 tagged with a C-terminal c-Myc epitope (Ste7me), cells were transformed, respectively, with pNC250 (a 2μm DNA plasmid containing the *URA3* gene and the *STE7* gene under control of the *CYC1* promoter) or with pNC267 (the same vector expressing the epitope-tagged *STE7* allele) (99). To overproduce Kss1 and Fus3, cells were transformed, respectively, with YEpT-*KSS1* (a 2μm DNA plasmid carrying the *KSS1* gene and the *TRP1* gene) or with YEpT-*FUS3* (the same vector carrying the *FUS3* gene) (gifts of D. Ma, this laboratory). To construct YEpT-*KSS1*, an *Eco*RI-*Sph*I fragment containing *KSS1* and its promoter were excised from plasmid YEp-*KSS1* (59) and inserted into the corresponding sites of YEp352-TRP, a derivative of YEp352 (43) in which the *URA3* gene was replaced with the *TRP1* gene (constructed by K. Kuchler, this laboratory). YEpT-*FUS3* was constructed in a similar fashion, using a *Bam*HI-*Sal*I fragment containing *FUS3* and its promoter that had been excised from plasmid pYEE81 (28). YEpT-*KSS1*(*K42R*), containing K42R Q45P substitution mutations (indicated as one-letter code for original amino acid followed by position number followed by one-letter code for amino acid to which the original amino acid was changed) that inactivate catalytic activity, and YEpT-*KSS1*(*AEF*), containing T183A Y185F substitution mutations that prevent phosphorylation and activation (designated AEF), were constructed by inserting *Eco*RI-*Sph*I fragments excised from, respectively, plasmids YEp-K42R Q45P and YEp-T183A Y185F (59) into the corresponding sites of YEplac112 (a *TRP1*-containing 2μm DNA plasmid) (37). YEpU-*KSS1*(Δ*loop*) was constructed by excising an *Eco*RI-*Sph*I fragment containing this allele from phage M13-*KSS1*(Δ*loop*) and inserting it into the corresponding sites of the *URA3*-containing 2μm DNA vector, YEp352. To generate M13-*KSS1*(Δ*loop*), oligonucleotide-directed mutagenesis (65) was performed with a commercial kit (Amersham Corp.), using as the template M13-*KSS1* (which is M13 carrying a genomic *Eco*RI-*Sph*I fragment containing the *KSS1* gene; gift of D. Ma, this laboratory) and primer JGC3 (5′-GCCCTGTACCATCGCGTTCCGCATAATGTATAT GTGACGTCAGGTACCGACCTCGCAGTCCAAAAT-3′). In the *KSS1*(Δ*loop*) allele, codons 168 to 187 of *KSS1* are replaced with codons 236 to 245 of *TPK3* (91) and a substitution mutation (C167S) is also present. YEpUG-*KSS1*(*1-315*) (gift of D. Ma, this laboratory), expressing a 53-residue C-terminal truncation allele from the *GAL1* promoter, was derived from YEpGAL-*KSS1* (59). *KSS1*(*1-315*) was created by using oligonucleotide-directed mutagenesis to insert a G after codon 315 in the *KSS1* coding sequence, which causes a frameshift that generates a two-residue extension (Val-Pro) and then terminates the open reading frame (ORF) at a TGA. Low-copy-number (*CEN*-based) plasmids expressing various *STE7* alleles, specifically YCpT-*STE7*, YCpU-*STE7*, YCpT-*STE7*(*171-515*), YCpU-*STE7*(*171-515*), and YCpT-*STE7*(*23-515*), were generated in several steps. YCplac22Nco was constructed by inserting a double-stranded oligonucleotide, generated by annealing LB50 (5′-GATCCCAATTGCCACCATTGTCTA GAG-3′) with LB51 (5′-CTGACTCTAGACCATGGTGGCAATTGG-3′) into YCplac22 (37) that had been cut with *Bam*HI and *Sal*I. The *STE7* promoter and its upstream region (nucleotides 5 to 350 [90]) were amplified by the PCR with genomic DNA as the template and primers STE7P-N (5′-CGCGGTACCTTGT GGTCTTAAAAGAATGTG-3′) and STE7P-C (5′-CGCGGATCCAATATAC CACGCTGCAAAA-3′). The resulting product was digested with *Kpn*I and *Bam*HI and inserted into the corresponding sites of YCplac22Nco, yielding YCpT-*STE7P*. To construct YCpT-*STE7*, a *Bam*HI-*Hin*dIII fragment (containing the *STE7* coding sequence) was excised from pNC279 (99) and inserted into the corresponding sites in YCpT-*STE7P*. To construct YCpT-*STE7*(*171-515*), a *Bam*HI-*Hin*dIII fragment (carrying the *STE7*(*171-515*) allele) was excised from pGEM4Z-*STE7*(*171-515*) (see below) and inserted into the corresponding sites of YCpT-*STE7P*. To construct YCpT-*STE7*(*23-515*), an *Nco*I-*Hin*dIII fragment carrying the *STE7*(*23-515*) allele was excised from pGEM4Z-*STE7*(*23-515*) (see below) and inserted into the corresponding sites of YCpT-*STE7P*. YCpU-*STE7* and YCpU-*STE7*(*171-515*) were constructed by inserting *Kpn*I-*Hin*dIII fragments from, respectively, YCpT-*STE7* and YCpT-

TABLE 1. *S. cerevisiae* strains used in this study

Strain	Genotype	Source or reference
DC17	*MAT*α *his1*	J. B. Hicks
BJ2168	*MAT***a** *leu2 trp1 ura3-52 prb1-1112 pep4-3 prc1-407 gal2*	47
YPH499	*MAT***a** *ade2-101^{oc} his3-Δ200 leu2-Δ1 lys2-801^{am} trp1-Δ1 ura3-52*	81
YDM230	YPH499 *kss1*Δ::*hisG fus3-6*::*LEU2*	59
E929-6C	*MAT***a** *cyc1 CYC7-H2 can1 leu2-3,112 trp1-Δ1 ura3-52*	21
E929-6C-1	E929-6C *ste7-Δ3*::*LEU2*	21
SY1390	*MAT*α *FUS1*::*HIS3 leu2 ura3 trp1 his4-519 his3-Δ200*::*ura3 pep4*::*ura3 can1*	88
SY1492	SY1390 *ste5*::*LEU2*	88
YLB103	SY1390 *ste5*::*LEU2 ste11*::*hisG*	This work

STE7(*171-515*) into the corresponding sites of YCplac33 (a *CEN*- and *URA3*-containing vector) (37). YCpT-*STE7* and YCpU-*STE7* restore a wild-type level of mating proficiency to a *ste7*Δ strain (E929-6C-1). pJD11, containing eight tandem consensus pheromone response elements (PREs; Ste12-binding sites) driving a *lacZ* reporter gene, has been described before (23).

***E. coli* expression vectors and plasmids for in vitro transcription.** pGEX-*STE7*(*1-172*), a bacterial expression vector that produces a chimeric protein in which the first 172 N-terminal residues of Ste7 (plus an extension of five extraneous residues) are fused to the C terminus of *Schistosoma japonicum* glutathione *S*-transferase (GST) through a 15-amino-acid spacer (that includes a thrombin cleavage site), was constructed as follows. pYGU-*STE7* (14) was cleaved with *Bgl*II, and the resulting 5′ overhang was filled in with the Klenow fragment of *E. coli* DNA polymerase I. This intermediate was then digested with *Xho*I, and the resulting *Xho*I-blunt-ended fragment (containing codons 1 to 172 of *STE7*) was inserted into pGEX-5X-2 (Pharmacia) that had been cut with *Not*I, filled in, and then cleaved with *Sal*I. pBS-*ERK2*, containing the rat ERK2 cDNA in pBluescript SK$^-$ (Stratagene) in the T3 orientation, has been described elsewhere (11). pBS-*FUS3* contains the *FUS3* ORF inserted into pBluescript SK$^+$ (Stratagene) in the T3 orientation, and pBS-T7*MPK1* contains the *MPK1* ORF inserted into pBluescript SK$^+$ in the T7 orientation (gifts of C. Inouye, this laboratory). To fuse Fus3 to an N-terminal c-Myc epitope tag, creating meFus3, an *Eco*RI-*Bam*HI fragment containing the *FUS3* ORF was inserted into the corresponding sites in pGEM4Z-9E10 (4), yielding pGEM4Z-*meFUS3*, in which the N-terminal sequence is MEQKLISEEDLEFT**M**- (epitope tag underlined, native Fus3 initiator Met in boldface). pGEM4Z-*KSS1*, pGEM4Z-*KSS1*(*AEF*), and pGEM4Z-*KSS1*(*1-315*) were constructed by inserting the corresponding *Bam*HI-*Sph*I fragments from YEpGAL-*KSS1*, YEp-T183A Y185F, and YEpUG-*KSS1*(*1-315*) into pGEM4Z (Promega Biotec) that had been cleaved with the same restriction enzymes. pGEM4Z-*KSS1*(Δ*loop*) was constructed by replacing the *Eco*RV-*Sph*I fragment of pGEM4Z-*KSS1* with the corresponding fragment from YEpU-*KSS1*(Δ*loop*). pGEM4Z-*STE7* was constructed by inserting the *Kpn*I-*Hin*dIII fragment from pYGU-*STE7* into the corresponding sites of pGEM4Z. pGEM4Z-*STE7*(*171-515*) was constructed by replacing the *Eco*RI-*Bgl*II fragment in pGEM4Z-*STE7* with a double-stranded oligonucleotide, generated by annealing LB54 (5′-AATTCGGATCCAAC**ATG**GCA-3′; start codon in boldface, codon 171 of *STE7* underlined) with LB55 (5′-GATCTGCCATGTTG GATCCG-3′). PCR was used to amplify codons 23 to 135 of *STE7*, using plasmid pGEM4Z-*STE7* as the template and primers STE7-23-X (5′-GC*GAATTC*AC C**ATG**GTGGGCAATAATGGCCA-3′; introduced initiation codon in boldface, introduced *Eco*RI site in italics, and codon 23 of *STE7* underlined) and T7PL (5′-GCTCTAATACGACTCACTATAGGGAGA-3′). The product was digested with *Eco*RI, and the resulting 113-bp *Eco*RI fragment was used to replace the larger *Eco*RI fragment in pGEM4Z-*STE7*, generating pGEM4Z-*STE7*(*23-515*). pGEM4Z-SP6*STE12* was constructed by inserting an *Eco*RI fragment (containing *STE12*) excised from pGAD-*STE12* (gift of S. Fields) into the *Eco*RI site of pGEM4Z in the SP6 orientation. PCR was used to amplify the *HOG1* ORF, using plasmid pJB17 (12) as the template and primers HOG1-5′ (5′-GCGGGATCCACC**ATG**ACCACTAACGAGGAATTCATTAGGA-3′; introduced *Bam*HI site underlined, *HOG1* start codon in boldface) and HOG1-3′ (5′-CGGCGGATCCACGTCCACTTTACTTTGTAATTGAG-3′; *Bam*HI site underlined). The product was digested with *Bam*HI and inserted in the SP6 orientation into the *Bam*HI site of either pGEM-4Z or pGEM4Z-9E10, yielding pGEM4Z-SP6*HOG1* and pGEM4Z-*meHOG1*, respectively. The latter plasmid encodes a c-Myc epitope-tagged Hog1 with the N-terminal sequence MEQKLI SEEDLEFT**M** (epitope tag underlined, native Hog1 initiator Met in boldface). PCR was also used to amplify the *PBS2* ORF, using plasmid YEp24.*PBS2* (10) as the template and primers PBS2-5′ (5′-GCGGGATCCACC**ATG**GAAGAC AAGTTTGCTAACCTCA-3′; introduced *Bam*HI site underlined, *PBS2* start codon in boldface) and PBS2-3′ (5′-CGGCGGATCCATCCCCTCAATA CTCTGTCATAA; *Bam*HI site underlined). The product was digested with *Bam*HI and inserted into the *Bam*HI site of pGEM4Z-9E10 in the T7 orientation, generating pGEM4Z-T7*PBS2*.

Transcription and translation in vitro. Most templates for in vitro transcription, encoding the indicated proteins, were prepared from the plasmid DNAs indicated by linearization with the restriction endonucleases specified, followed by extraction with phenol-chloroform-isoamyl alcohol (25:24:1) and filtration through a Sepharose CL-4B (Pharmacia) spin column: Ste12, pGEM4Z-SP6*STE12*, *Ssp*I; Erk2, pBS-*ERK2*, *Hin*dIII; Mpk1, pBS-T7*MPK1*, *Eco*RI; Hog1, pGEM4Z-SP6*HOG1*, *Hin*dIII; meHog1, pGEM4Z-*meHOG1*, *Hin*dIII; Pbs2, pGEM4Z-T7*PBS2*, *Eco*RI; Ste7, pGEM4Z-*STE7*, *Hin*dIII; $Ste7_{1-172}$, pGEM4Z-*STE7*, *Bgl*II; $Ste7_{23-515}$, pGEM4Z-*STE7*(*23-515*), *Hin*dIII; $Ste7_{171-515}$, pGEM4Z-*STE7*(*171-515*), *Hin*dIII; Kss1, pGEM4Z-*KSS1*, *Nde*I; $Kss1_{AEF}$, pGEM4Z-*KSS1*(*AEF*), *Nde*I; $Kss1_{\Delta loop}$, pGEM4Z-*KSS1*(Δ*loop), Nde*I; $Kss1_{1-356}$, pGEM4Z-*KSS1*, *Nsp*I; $Kss1_{1-344}$, pGEM4Z-*KSS1*, *Bsp*EI; $Kss1_{1-315}$, pGEM4Z-*KSS1*(*1-315*), *Nde*I; $Kss1_{1-272}$, pGEM4Z-*KSS1*, *Nco*I; and, $Kss1_{1-105}$, pGEM4Z-*KSS1*, *Ase*I. Certain templates for in vitro transcription, encoding the indicated proteins, were generated by PCR from the templates and using the primers given, then extracted with phenol-chloroform-isoamyl alcohol (25:24:1), and filtered through Sepharose CL-4B in a spin column: $Ste7_{1-477}$, pGEM4Z-*STE7*, SP6 P/P (5′-GATTTAGGTGACACTATAGA-3′) plus STE7-X-477 (5′-CG GTCGACTATTTATCATCTTTAGACGG-3′); $Ste7_{1-278}$, pGEM4Z-*STE7*, SP6 P/P plus STE7-X-278 (5′-CGGTCGACTAAGAACCACAATCAGAGTA-3′); $Ste7_{1-98}$, pGEM4Z-*STE7*, SP6 P/P plus STE7-X-98 (5′-GGCTACAGATCTAC TAAAACAGGTTCATTTTG-3′); $Ste7_{46-515}$, pGEM4Z-*STE7*, T7PL plus STE7-46-X (5′-GCGAATTCACCATGGTGATGTCTAACATTAATG-3′); $Ste7_{98-515}$, pGEM4Z-*STE7*, T7PL plus STE7-98-X (5′-GCGAATTCACCATGGTTCT GTCTTCTCTATCA-3′); and, $Kss1_{97-368}$, pGEM4Z-*KSS1*, T7PL plus KSS1-97-X (5′-GCGAATTCACCATGGAAACCGATTTACAAA-3′). To incorporate an SP6 RNA polymerase promoter into the PCR products encoding $Ste7_{46-515}$, $Ste7_{98-515}$, and $Kss1_{97-368}$, a second round of PCR was performed with 1 μl of the initial PCR mixture as the template, the downstream primer from the initial reaction, and primer SP6EP (5′-GATTTAGGTGACACTATAGAGCGAATT CACCATG-3′), which contains an SP6 promoter and is identical to the upstream primer from the initial reaction in the sequence underlined. Transcription and translation reactions in vitro were performed as described previously (6). Briefly, RNAs synthesized by SP6, T3, or T7 bacteriophage RNA polymerase (Promega Biotec) from linear DNA templates (see above) were purified and used to program an mRNA-dependent rabbit reticulocyte lysate (Novagen). To radiolabel, translation reactions were performed in the presence of [^{35}S]Met (Dupont NEN). Protein yield was calculated from the percent incorporation of [^{35}S]Met into protein, the known number of Met residues in each polypeptide, and the specific radioactivity of the label, correcting for isotope dilution by the concentration of endogenous Met in the lysate. The latter was determined for each batch of lysate by adding a trace amount of [^{35}S]Met to a sample of the lysate, then conducting translation reactions in the presence of increasing amounts of exogenously added nonradioactive Met, and observing the concentration of added Met required to reduce the incorporation of label into protein by 50%. Prior to their use in coimmunoprecipitation studies, translation products were concentrated and partially purified by ammonium sulfate precipitation as described previously (6).

Buffers, protein production, and analysis. The following solutions were used for the purposes indicated. Buffer A (immunoprecipitation of proteins translated in vitro) was 125 mM potassium acetate, 4 mM $MgCl_2$, 0.5 mM EDTA, 1 mM dithiothreitol (DTT), 0.1% (vol/vol) Tween 20, 12.5% (vol/vol) glycerol, and 20 mM Tris-HCl (pH 7.2); buffer B (lysis of yeast cells and immunoprecipitation of proteins from cell extracts) was the same as buffer A except that $MgCl_2$ was omitted and 0.5 mM ethylene glycol-bis(β-aminoethyl ether)-*N*,*N*,*N*′,*N*′-tetraacetic acid (EGTA), 1 mM 4-(2-aminoethyl)-benzenesulfonylfluoride (Calbiochem), 1 mM sodium orthovanadate, 25 mM β-glycerophosphate, and 10 μg of pepstatin A per ml were added; buffer C (assay of protein kinase activity) was the same as buffer B except that 12 mM $MgCl_2$ and 1 mg of bovine serum albumin (BSA) per ml were present, DTT was raised to 2 mM, glycerol was lowered to 5% (vol/vol), sodium orthovanadate was lowered to 0.5 mM, and β-glycerophosphate was lowered to 12.5 mM. Conventional methods were used for measurement of total protein concentration, for sodium dodecyl sulfate (SDS)-polyacrylamide gel electrophoresis (PAGE), for immunoblotting, and for purification of bacterially expressed proteins (26, 39). SDS-PAGE sample buffer was 2 mM EDTA, 1% (wt/vol) DTT, 6% (wt/vol) SDS, 20% (vol/vol) glycerol, 0.05% (wt/vol) bromphenol blue, and 200 mM Tris-HCl (pH 6.8). The rabbit polyclonal antisera used for analysis of Kss1 (59), Fus3 (13), and Ste7 (14) are described in the citations given. The mouse monoclonal antibody (MAb) that recognizes the c-Myc epitope (9E10) used in this work has been described elsewhere (34). Detection of immune complexes was performed by using a commercial chemiluminescence system (ECL; Amersham).

Preparation of yeast cell extracts, immunoprecipitation, and protein kinase assays. Yeast strains were grown at 30°C with rotary shaking in selective medium (40 ml) to mid-exponential phase (A_{595} of ~0.8). When untreated and pheromone-stimulated cultures were compared, cells were harvested by centrifugation, resuspended at an A_{595} of ~2 in two equal portions in fresh medium that was buffered with 25 mM sodium succinate (pH 3.5) to impede pheromone proteolysis (18), and incubated on the shaker for 15 min to permit recovery from the prior manipulations. One portion was treated with α-factor (Peninsula Laboratories or Star Biochemicals) at a final concentration of 12 μM, the other was left untreated, and both were incubated for an additional 15 min. Thereafter, the cells were chilled rapidly in an ice-water slurry, collected by centrifugation, washed with ice-cold phosphate-buffered saline (10 ml), resuspended in a 0.5-ml microcentrifuge tube in buffer B (0.2 ml), and lysed by vigorous vortex mixing with 0.2 g of glass beads (0.45- to 0.6-mm diameter) for six 30-s periods (separated by 1-min periods of cooling on ice). The lysate was clarified by centrifugation for 5 min at 13,000 × *g* at 4°C. The resulting crude extract was used immediately for immunoprecipitation experiments. Prior to incubation with antigen, antibodies were prebound to a mixture of protein A and protein G immobilized on agarose beads (hereafter designated protein A/G-agarose beads) (Oncogene Science) by incubating (for each immunoprecipitation reaction) 0.5 to 2 μl of the appropriate antiserum (or ascites fluid) with 15 μl of a suspension (50%) of the protein A/G-agarose beads. The amount of antibody bound was that sufficient to immunoprecipitate 20 to 40% of the antigen (~5 nM) present in a standard reaction mixture (0.2 ml) in a 1.5-ml tube. When the antigen was a protein produced by in vitro translation, the indicated quantity (see figure legends) of each partially purified translation product was added to buffer A (0.2 ml), incubated for 30 min at 30°C, used to resuspend the appropriate antibody-protein A/G-agarose complexes, and incubated for an additional 1 h at room temperature on a roller drum. The beads were allowed to settle by gravity, and the supernatant solution was removed. The beads were then washed three times

with 1 ml of ice-cold buffer A, with collection by centrifugation at maximum speed in a microcentrifuge for 2 s. Bound proteins were solubilized in 30 μl of SDS-PAGE sample buffer, resolved by SDS-PAGE, and visualized by fluorography using a commercial fluorography reagent (Amplify; Amersham). For the reaction $A + B \leftrightarrow AB$, $K_d \equiv ([A]_{eq} \times [B]_{eq})/[AB]_{eq}$, where $[A]_{eq} = ([A]_0 - [AB]_{eq})$, $[B]_{eq} = ([B]_0 - [AB]_{eq})$, and $[A]_0$ and $[B]_0$ are the input concentrations of A and B. $[AB]_{eq}$ is the percentage of B coprecipitated with A divided by the percentage of A precipitated by the antibody and multiplied by $[B]_0$.

When the antigen was a protein in a yeast cell extract, extract (1 mg of total protein) in buffer B (0.2 ml) was precleared by incubation with 20 μl of a suspension (50%) of protein A/G-agarose beads for 15 min at 4°C on a roller drum. The beads and any residual insoluble material were removed by centrifugation for 5 min at 13,000 × *g* at 4°C. The resulting supernatant solution was incubated for 30 min at 4°C with the appropriate antibody-protein A/G-agarose complexes on a roller drum. The beads were collected and washed in ice-cold buffer B as described above. Bound proteins were eluted and subjected to SDS-PAGE as described above and visualized by immunoblot analysis. Phosphotransferase activity of protein kinases was measured in immune complexes as follows. Antigen-antibody-protein A/G complexes were prepared as described above except that 30 μl of antibody-protein A/G-agarose beads was added in each reaction and the final wash was omitted. After the second wash, the beads were resuspended in buffer C (0.6 to 0.8 ml), and the resulting slurry was divided into three or four equal portions (0.2 ml each). The beads were collected by centrifugation, and the supernatant solution was removed by aspiration. The bead pellets were placed on ice, and one aliquot was suspended in SDS-PAGE sample buffer for later immunoblot analysis. The remaining aliquots were overlaid with 10 μl of buffer C containing 10 μM [γ-^{32}P]ATP (100 μCi/μmol), in the absence or presence (where indicated) of an exogenous substrate (see figure legends). The reaction was initiated by thorough mixing and transfer of the tubes to a 30°C water bath. After incubation for 4 min, reactions were terminated by addition of SDS-PAGE sample buffer (20 μl). In an experiment in which the distribution of proteins after the reaction was examined (see Fig. 7), prior to quenching, the beads were collected by centrifugation and the supernatant solution was removed mixed with SDS-PAGE sample buffer (15 μl). The beads were washed twice with ice-cold buffer B (1 ml) and then solubilized in 30 μl of SDS-PAGE sample buffer. Reaction products were resolved by SDS-PAGE and visualized by autoradiography.

Measurement of pheromone response. Three independent methods were used to assess the efficiency of pheromone action. For quantitative determination of pheromone-induced transcription, strain E929-6C-1 (Table 1) was cotransformed with reporter plasmid pJD11 and either YCplac33, YCpU-*STE7*, or YCpU-*STE7*(*171-515*). The resulting transformants were grown to mid-exponential phase, treated with 12 μM α-factor pheromone for 1 h, harvested by centrifugation, and assayed for β-galactosidase activity as described elsewhere (23). An agar diffusion (halo) bioassay was used to measure pheromone-induced growth arrest and recovery as described previously (48, 75). For quantitative measurement of mating proficiency (86), 10^7 exponentially growing cells of the haploid strain to be examined (either E929-6C or E929-6C-1) carrying plasmid YCplac22, YCpT-*STE7*, YCpT-*STE7(171-515)*, or YCpT-*STE7(23-515)* were mixed with a 10-fold excess of cells of the opposite mating type (strain DC17), collected on a nitrocellulose filter, rinsed once with rich medium (YPD) (80), and incubated on the filter on a YPD plate at 30°C for 4 h. To score the number of prototrophic diploids formed in this time period, the cells were eluted from the filters, dispersed by vigorous vortex mixing in sterile water, and plated, at various dilutions, on synthetic medium lacking histidine and uracil. After 2 days of growth, the number of His^+ Ura^+ colonies was counted. Mating efficiency was defined as the number of diploids formed divided by the number of input haploids of the strain tested.

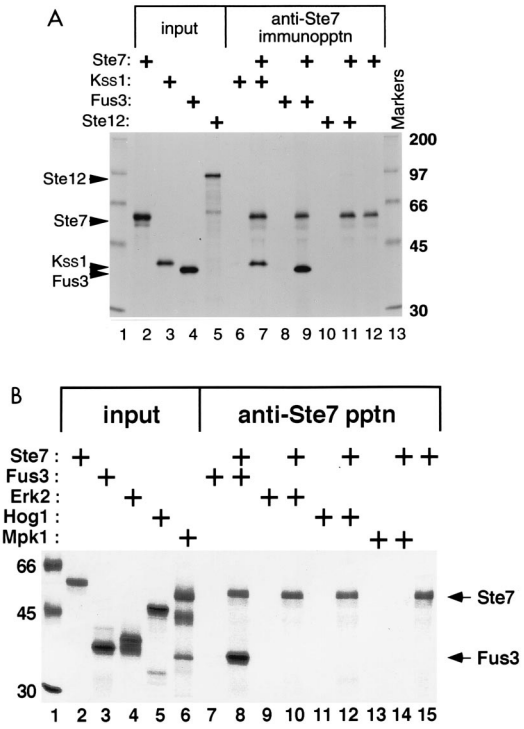

FIG. 1. Binding and specific recognition of Kss1 and Fus3 by Ste7 in vitro. (A) Ste7, Kss1, Fus3, and Ste12 were synthesized in vitro and partially purified by ammonium sulfate precipitation, and portions (for Kss1, Fus3, and Ste12, 5% of the amount added in the immunoprecipitation [immunopptn] reactions, and for Ste7, 25%; input) were subjected to SDS-PAGE in a 10% polyacrylamide gel (lanes 2 to 5). Samples (1 pmol) of the same proteins, each accompanied by ~60 μg of total protein from the rabbit reticulocyte lysate, were immunoprecipitated with anti-Ste7 antibodies either in the absence (lanes 6, 8, and 10) or in the presence (lanes 7, 9, 11, and 12) of 1 pmol of Ste7, and the resulting immunoprecipitates were analyzed on the same gel. Marker proteins of the indicated molecular masses (in kilodaltons) were also resolved on the same gel (lanes 1 and 13). (B) Ste7, Fus3, Erk2, Hog1, and Mpk1 were prepared as described above, and portions (for Fus3, Erk2, Hog1 and Mpk1, 5% of the amount added into the immunoprecipitation reactions, and for Ste7, 25%; input) and analyzed by SDS-PAGE as for panel A (lanes 2 to 6). Samples (1 pmol) of the same proteins were immunoprecipitated as for panel A with anti-Ste7 antibodies either in the absence (lanes 7, 9, 11, and 13) or in the presence of 1 pmol of either radiolabeled Ste7 (lanes 8, 10, 12, and 15) or nonradioactive Ste7 (lane 14), and the resulting immune complexes were analyzed in the same gel. Because of the similar electrophoretic mobilities of Ste7 and Mpk1, unlabeled Ste7 was used to permit unambiguous visualization of Mpk1. Molecular weight standards (lane 1) were as in panel A.

RESULTS

High-affinity and specific association of Kss1 and Fus3 with Ste7 in vitro. To assess the interaction between either Kss1 or Fus3 and their immediate upstream activator, Ste7, we used coimmunoprecipitation of the radiolabeled proteins prepared by sequential transcription and translation in vitro (6) as described in Materials and Methods. The virtues of this technique are that known amounts of protein can be examined in solution at low concentration under conditions such that nonspecific associations are minimized (as a result of the presence of an ~1,000-fold excess of unlabeled protein from the reticulocyte lysate) and in the absence of any other yeast proteins.

Ste7, Kss1, Fus3, and Ste12 were all efficiently produced in radiolabeled form under the conditions used (Fig. 1A, input). As expected, Ste7 protein was immunoprecipitated by the anti-Ste7 antiserum (Fig. 1A, lanes 7, 9, 11, and 12), whereas the Kss1, Fus3, and Ste12 proteins alone were not (Fig. 1A, lanes 6, 8, and 10). However, when Ste7 was present, both Kss1 and Fus3 were effectively coprecipitated (Fig. 1A, lanes 7 and 9), whereas Ste12 was not (Fig. 1A, lane 11). The ability of Kss1 and Fus3 to coprecipitate with Ste7 is indicative of a direct physical interaction between these proteins. When determined as described in Materials and Methods, the K_d for both the Kss1-Ste7 and the Fus3-Ste7 complex (at physiological temperature) was found to be ~5 nM. This value may be a minimum estimate of the binding affinity under these conditions because it is possible that some of the antibody species in the polyclonal antiserum interfered with the interaction and because some of the complexes may have dissociated during the wash steps, even though very brief washes with ice-cold buffer were used.

Recognition of Kss1 and Fus3 by Ste7 is highly specific. To determine if the binding of MAPKs to Ste7 was specific for Kss1 and Fus3, the abilities of two other yeast MAPKs, Hog1 (12) and Mpk1 (56), as well as a mammalian MAPK, Erk2

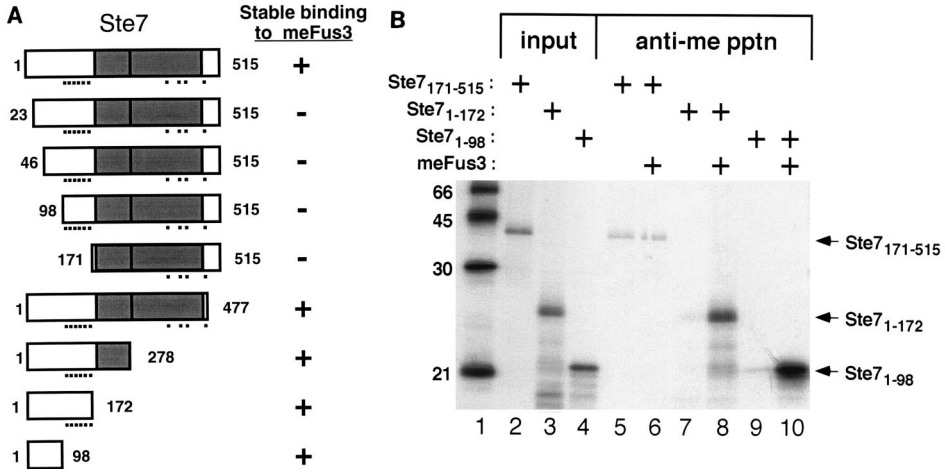

FIG. 2. Mapping of the Fus3-binding domain of Ste7. (A) Shown schematically are the various Ste7 derivatives constructed (open rectangles), with the first and last residues of each indicated by the numbers given. The position of the kinase catalytic core (grey box), subdivided (vertical bar) into its ATP-binding (left) and substrate-binding (right) domains (89), is also shown. The location of each of 10 S/TP sequences (small black boxes), which are potential target sites for MAPK phosphorylation (24), is indicated below each rectangle. The column to the right summarizes the results of experiments performed as for panel B. +, coprecipitated with meFus3; −, no significant coprecipitation above the background observed in the absence of meFus3. (B) Three of the various truncated Ste7 derivatives shown in panel A were prepared in radioactive form, meFus3 was prepared in nonradioactive form as described in the legend to Fig. 1, and portions of the Ste7 derivatives (5% of the amount added to the immunoprecipitation [pptn] reactions; input) were subjected to SDS-PAGE in a 15% polyacrylamide gel (lanes 2 to 4). Samples (2 pmol) of the same radiolabeled proteins, accompanied by ~80 μg of total protein from the rabbit reticulocyte lysate, were immunoprecipitated with the anti-c-Myc MAb 9E10 either in the absence (lanes 5, 7, and 9) or in the presence (lanes 6, 8, and 10) of 2 pmol of nonradioactive meFus3, and the resulting immune complexes were analyzed in the same gel. Marker proteins of the indicated molecular masses (in kilodaltons) were also resolved on the same gel (lane 1).

(11), to associate with Ste7 were examined by the same method. All three of these MAPKs were efficiently synthesized in the in vitro transcription-translation system (Fig. 1B, input). However, despite the fact that Hog1, Mpk1, and Erk2 are very similar in overall structure to Kss1 and Fus3 and have ~50% amino acid identity with Kss1 and Fus3 in their catalytic domains (about the same degree of amino acid identity that Kss1 and Fus3 have with each other), none of these three MAPKs coimmunoprecipitated with Ste7 (Fig. 1B, lanes 10, 12, and 14) under conditions in which Fus3 (Fig. 1B, lane 8) and Kss1 (not shown) did.

These results were confirmed with different antigen-antibody combinations. Ste7 bound to meFus3 (see Materials and Methods) but not to meHog1. Pbs2 (the MEK for Hog1) did not bind to meFus3. Similarly, Ste7, but not Pbs2, bound to Kss1 (data not shown).

The N-terminal 98 residues of Ste7 are necessary and sufficient for tight binding to Fus3. To localize the region of Ste7 responsible for its high-affinity interaction with Fus3 and Kss1, a series of Ste7 polypeptides truncated from either the N- or the C-terminal end was prepared and tested for the ability to bind to meFus3. As summarized schematically in Fig. 2A and illustrated for representative data in Fig. 2B, a fragment containing the C-terminal two-thirds of Ste7 (residues 171 to 515), which corresponds to its protein kinase catalytic core (38), was unable to bind stably to meFus3. Conversely, a fragment representing the noncatalytic N terminus (residues 1 to 172) and lacking the entire kinase domain of Ste7 coimmunoprecipitated with meFus3 with an affinity comparable to that displayed by full-length Ste7. Thus, the catalytic domain of Ste7 was completely dispensable for its high-affinity association with meFus3.

Both Fus3 (33) and Kss1 (as shown below) can phosphorylate Ste7 in vitro. Evidence from in vivo studies suggests that these phosphorylations may represent a physiologically significant negative feedback control on Ste7 activity (35, 59, 99). MAPKs are proline-directed protein kinases; the minimal consensus phosphorylation site consists of a Ser or Thr followed by a Pro (S/TP) (24). Ste7 contains 10 S/TP sites, 6 of which are clustered within the noncatalytic N terminus (residues 105 to 168). However, a fragment of Ste7 containing all 10 S/TP sites (residues 98 to 515) did not bind to meFus3 detectably (Fig. 2A). In marked contrast, a fragment of the N terminus (residues 1 to 98) devoid of any S/TP sites associated strongly with meFus3 (Fig. 2B), indicating that the putative target residues in Ste7 for MAPK phosphorylation neither are required for nor constitute the high-affinity binding site for Fus3. Conversely, removal of as few as 22 residues from the noncatalytic N terminus of Ste7 eliminated its ability to interact detectably with meFus3 (Fig. 2A). Thus, sequences within the first 98 residues of Ste7 were both necessary and sufficient to mediate the high-affinity interaction between Ste7 and Fus3.

Kss1 also associates with the N-terminal third of Ste7 (see below). This result and other similarities in the properties of Ste7-Kss1 and Ste7-Fus3 complexes, including similarities in K_d (see above), half-life (see below), and nature of binding (see below), suggest that Kss1 and Fus3 bind to the same site on Ste7 and, thus, that the binding of Kss1 and the binding of Fus3 to Ste7 are most likely mutually exclusive, although further experiments will be required to definitively establish this point.

The phosphoacceptor loop of Kss1 is not required for its high-affinity interaction with Ste7. Both Fus3 (35) and Kss1 (59) are phosphorylated by Ste7 on both a Tyr and a Thr residue in a -TEY- sequence located in the T loop (64) situated between conserved protein kinase subdomains VII and VIII (38). Likewise, all other MAPKs examined are also phosphorylated by their MEKs at equivalent TXY sequences in their T loops (19). This dual phosphorylation is absolutely required for activation of all MAPKs studied (1, 61), including Fus3 (35) and Kss1 (59). To determine whether the TEY site was necessary for the association of Kss1 and Ste7, a mutant version of Kss1, in which the TEY sequence was replaced with AEF (Fig. 3A), was tested (Fig. 3B) for its ability to associate with Ste7. This mutant protein still coimmunoprecipitated with Ste7, in-

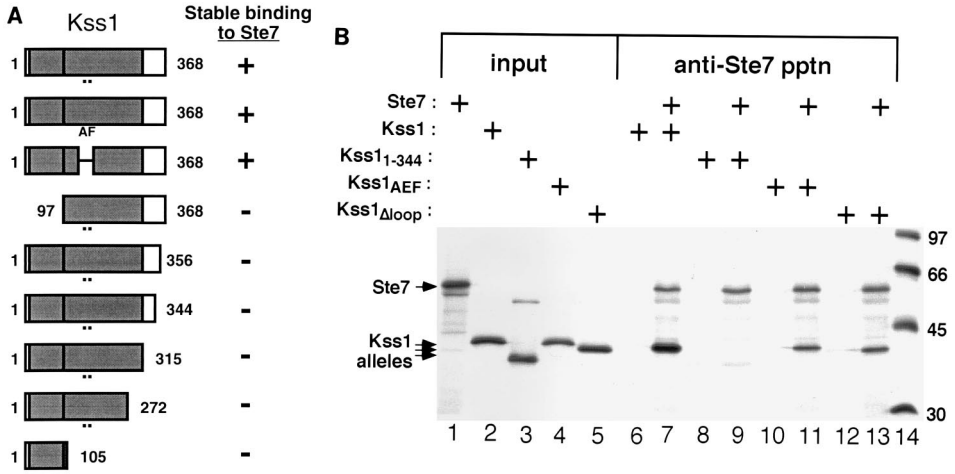

FIG. 3. The phosphoacceptor sites in Kss1 are not required for its tight binding to Ste7. (A) Shown schematically are the various Kss1 derivatives constructed (open rectangles), with the first and last residues of each indicated by the numbers given. The position of the kinase catalytic core (grey box), subdivided (vertical bar) into its ATP-binding (left) and substrate-binding (right) domains (89), is also shown. Locations of Thr-183 and Tyr-185 (small black boxes), which are the target residues in Kss1 for its phosphorylation and activation by Ste7 in vivo (59), are indicated below each rectangle, except in the second derivative ($Kss1_{AEF}$), in which these residues were mutated to Ala (A) and Phe (F), respectively, and the third derivative ($Kss1_{\Delta loop}$), in which they were deleted. The column to the right summarizes the results of experiments performed as for panel B. +, coprecipitated with Ste7; −, no significant coprecipitation above the background observed in the absence of Ste7. (B) Ste7, Kss1, and three of the various Kss1 derivatives shown in panel A were prepared in radioactive form as described in the legend to Fig. 1, and portions (for Kss1 and the Kss1 derivatives, 5% of the amount added to the immunoprecipitation [pptn] reactions and, for Ste7, 25%; input) were subjected to SDS-PAGE in a 10% polyacrylamide gel (lanes 1 to 5). Samples (1 pmol) of the same radiolabeled proteins, accompanied by ~80 μg of total protein from the rabbit reticulocyte lysate, were immunoprecipitated with the anti-Ste7 antibodies either in the absence (lanes 6, 8, 10, and 12) or in the presence (lanes 7, 9, 11, and 13) of 1 pmol of Ste7, and the resulting immune complexes were analyzed in the same gel. Marker proteins of the indicated molecular masses (in kilodaltons) were also resolved on the same gel (lane 14).

dicating that the Tyr and Thr residues of the phosphoacceptor site are not required for the high-affinity binding of Kss1 by Ste7. However, the catalytic clefts of protein kinases also interact with residues adjacent to (and to both the N and C sides of) the phosphoacceptor amino acid (89). To determine whether any portion of the T loop of Kss1 contributes to the recognition of Kss1 by Ste7, this entire 21-residue segment of Kss1 was removed and replaced with the 11-residue T loop of the *S. cerevisiae* Tpk3 protein (91), a homolog of the catalytic subunit of mammalian cyclic AMP-dependent protein kinase, which bears no sequence similarity to the T loop of Kss1 (or Fus3). This Kss1 derivative ($Kss1_{\Delta loop}$) also retained the ability to coimmunoprecipitate with Ste7 (Fig. 3B). Thus, in agreement with our observation that the catalytic domain of Ste7 is not required for its high-affinity association with Kss1, we found that the target site for phosphorylation of Kss1 by Ste7 is also not required for the tight interaction of these two proteins.

Nevertheless, it was noted that the apparent dissociation constant for the binding of both $Kss1_{AEF}$ and $Kss1_{\Delta loop}$ by full-length Ste7 was about 10-fold weaker than that for the interaction of Ste7 with native Kss1. This observation could indicate that residues in the T loop do contribute somewhat (~12% of the total) to the free energy of binding in the Ste7-Kss1 complex. Alternatively, however, perturbations of the T loop may have some subtle effect on the overall structure of Kss1 that influences binding affinity. A derivative of Kss1 lacking the entire ATP-binding lobe of its catalytic domain did not detectably coimmunoprecipitate with Ste7 (Fig. 3A). Removal of as few as 12 residues from the C terminus of Kss1 (Fig. 3A) also eliminated its association with Ste7. These deletions probably destabilize the structure of the remainder of the molecule (our unpublished observations).

Ste7-Fus3 and Ste7-Kss1 complexes can be isolated from extracts of naive and pheromone-stimulated cells. To assess the potential physiological significance of the tight binding observed in vitro between the MEK (Ste7) and the MAPKs (Fus3 and Kss1) of the pheromone response pathway, it was important to establish that such complexes could be detected when the proteins were produced in vivo. In our hands, the endogeous level of Ste7 is so low that it cannot be measured reliably by immunoblotting (16a). Hence, for in vivo studies, we expressed from multicopy plasmids either Ste7me (a fully functional version of Ste7 tagged at its C terminus with the c-Myc epitope [99]) or, as a control, native Ste7, along with either Fus3 or Kss1, in *MAT***a** cells that were either treated with α-factor mating pheromone or left untreated. As detected with polyclonal anti-Ste7 antibodies (Fig. 4, top panel, input), Ste7 migrated upon SDS-PAGE as a series of bands with apparent masses of 64 to 78 kDa, as has been observed previously (14, 99). The most rapidly migrating species comigrates with Ste7 produced by in vitro translation (data not shown); it has been shown elsewhere that the more slowly migrating forms of Ste7 are hyperphosphorylated species (14). Compared with Ste7 itself, the bands corresponding to Ste7me all have a slightly slower electrophoretic mobility, consistent with the extra mass contributed by the c-Myc epitope (Fig. 4, top panel). Prior treatment of cells with pheromone caused a shift of the Ste7me species to the more slowing migrating forms (Fig. 4, lane 3), indicative of activation of the pheromone response pathway, as reported previously (14, 99).

As expected, native Ste7 was not immunoprecipitated by the anti-c-Myc MAb (Fig. 4, lane 5). When the immunoprecipitates were analyzed with anti-Fus3 antibodies (Fig. 4, lower panel), it was found that Fus3 was absent from the Ste7 control lane but did effectively coimmunoprecipitate with Ste7me, regardless of whether the cells had been stimulated by pheromone. The fact that Fus3 can coprecipitate even with unactivated Ste7me from cell extracts is consistent with our observation that Ste7 translated in vitro (and, thus, most likely

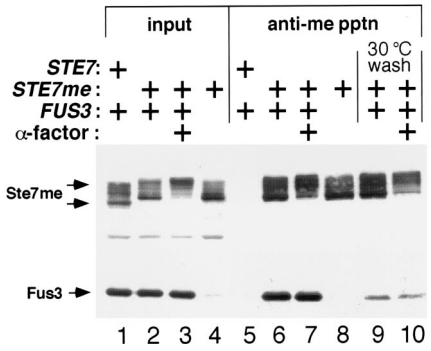

FIG. 4. Ste7-Fus3 complexes are present in extracts from naive and pheromone-treated cells. Cultures of strain BJ2168 (Table 1), expressing from a multicopy plasmid either Ste7 or Ste7me, with or without coexpression of Fus3 from a multicopy plasmid (as indicated), were grown, treated or not treated with α-factor (as indicated), and harvested. Cell extracts were prepared, and portions (5% of the amount added in the immunoprecipitation [pptn] reactions; input) were subjected to SDS-PAGE in a 10% polyacrylamide gel (lanes 1 to 4). Samples of the extracts were immunoprecipitated with the anti-c-Myc MAb 9E10 as described in Materials and Methods and then subjected to either three rapid washes with ice-cold buffer (lanes 5 to 8) or three 2-min washes at 30°C (lanes 9 and 10). The resulting immunoprecipitates were solubilized, resolved by SDS-PAGE, and analyzed by immunoblotting with a mixture of anti-Ste7 and anti-Fus3 antisera.

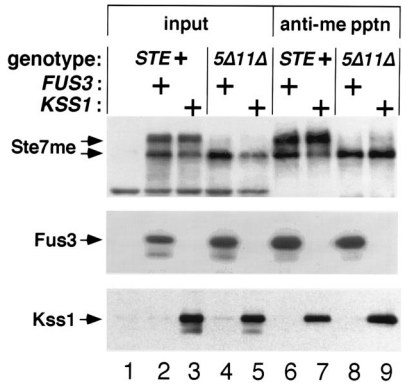

FIG. 5. Formation of Ste7-Kss1 and Ste7-Fus3 complexes does not require Ste5 or Ste11. Cultures of strain SY1390 (*STE*$^+$) or YLB103 (*ste5*Δ *ste11*Δ), carrying no plasmid (lane 1) or expressing Ste7me from a multicopy plasmid, with coexpression from a multicopy plasmid of either Fus3 or Kss1 (as indicated), were grown and harvested as described in Materials and Methods. Cell extracts were prepared, and portions (5% of the amount added to the immunoprecipitation [pptn] reactions; input) were subjected to SDS-PAGE in a 10% polyacrylamide gel (lanes 1 to 5). Samples of the extracts were immunoprecipitated with the anti-c-Myc MAb 9E10 (lanes 6 to 9) as described in Materials and Methods, using three rapid washes with ice-cold buffer. The resulting immunoprecipitates were solubilized, divided into three equal portions, resolved by SDS-PAGE, and analyzed by immunoblotting with either anti-Ste7 (top panel), anti-Fus3 (middle panel), or anti-Kss1 (bottom panel) antiserum.

unactivated) can interact strongly with either Kss1 or Fus3 that has been translated in vitro. In complementary experiments, native Ste7 was immunoprecipitated, and Kss1 or Fus3 was efficiently coimmunoprecipitated, by polyclonal anti-Ste7 antiserum (data not shown).

In the immunoprecipitation procedure used in this work, the bead-bound immune complexes were washed rapidly three times with an excess volume of ice-cold buffer as described in detail in Materials and Methods. Even when the incubation time for each wash was increased to 2 min and the temperature of each wash was raised to 30°C, a readily detectable amount of Fus3 was still present in the Ste7me immunoprecipitates (Fig. 4, lanes 9 and 10); however, the level of Fus3 bound was significantly reduced. By quantitating the degree of reduction of Fus3 (or Kss1) observed in several experiments of this type, a preliminary estimate for the apparent half-time for dissociation of either the Ste7me-Fus3 or the Ste7me-Kss1 complex at 30°C could be obtained and was approximately 2 to 3 min for both. Thus, although relatively stable, the Ste7-Fus3 and Ste7-Kss1 interaction is nonetheless reversible at physiological temperatures and, hence, potentially dynamic in the cell. The fact that the Ste7me-Fus3 and Ste7me-Kss1 association could be disrupted by such a mild treatment also demonstrated that the complexes were not a nonphysiological aggregate of denatured protein.

Formation of Ste7-Fus3 and Ste7-Kss1 complexes does not require Ste5 or Ste11. Ste5 protein has been shown to interact with Ste11, Ste7, Fus3, and Kss1 (17, 60, 72). Kss1 also interacts in the two-hybrid assay with Ste11 (17, 72). Because Ste11 phosphorylates Ste7, it must interact with this substrate (transiently or stably). These findings raised the possibility that the Ste7-Fus3 and Ste7-Kss1 interaction observed by coimmunoprecipitation from cell extracts might be mediated by bridging through Ste5 and/or Ste11. We considered both of these possibilities unlikely for two reasons. First, Ste7me and Fus3 (or Kss1) were overproduced in the cells used for the coimmunoprecipitation experiments, whereas both Ste5 (45a) and Ste11 (14) are not abundant proteins. Second, as described above, in vitro-translated Ste7 and Kss1 (or Fus3) bound with high affinity in the absence of added Ste5 or Ste11. Nevertheless, to definitively address this issue, the abilities of Kss1 and Fus3 to coimmunoprecipitate with Ste7me were examined in a *ste5*Δ *ste11*Δ double mutant and in an otherwise isogenic *STE5*$^+$ *STE11*$^+$ strain (Fig. 5). As expected, in the *ste5*Δ *ste11*Δ double mutant, little or no hyperphosphorylated Ste7me was observed, consistent with the requirement of Ste11 and Ste5 for signal transmission to Ste7 (99). Despite the total absence of both Ste5 and Ste11, Fus3 (Fig. 5, lanes 6 and 8) or Kss1 (lanes 7 and 9) still coimmunoprecipitated with Ste7me with an efficiency approximately equal to that observed in the extracts from wild-type cells (Fig. 5, lanes 6 and 8). These results are consistent with previous results showing that a Ste7-Fus3 two-hybrid interaction is maintained in strains with either *STE5* or *STE11* singly deleted (17, 72).

In the complex, both Ste7 and Kss1 are catalytically active. To examine the protein phosphotransferase activities present in isolated Ste7-MAPK complexes, Ste7me was overproduced in either a wild-type *MAT***a** strain or an otherwise isogenic *kss1*Δ *fus3*Δ double mutant. Complexes were isolated both from unstimulated cells and from cells that had been stimulated by brief treatment (15 min) with α-factor, and the complexes were incubated with [γ-^{32}P]ATP · Mg^{2+} at 30°C for 4 min.

In the reaction containing immune complexes isolated from wild-type cells, the most prominent phosphoprotein had an apparent molecular mass of ~75 kDa (Fig. 6A, lane 1), in agreement with the mobility expected for phosphorylated Ste7me. Incorporation of ^{32}P into this species was stimulated by prior treatment of the cells with α-factor pheromone (Fig. 6A, lane 2) and was abolished when Ste7me was immunoprecipitated from the *fus3*Δ *kss1*Δ mutant (Fig. 6A, lanes 3 and 4). Since it has been shown that Ste7 is phosphorylated in a Fus3-dependent and pheromone-stimulated manner (33), these results confirmed the identification of the ~75-kDa radiolabeled band as Ste7me.

The immunoprecipitates isolated from wild-type cells potentially contained both Ste7me-Fus3 and Ste7me-Kss1 complexes; however, the protein kinase activity of Kss1 in vitro has not

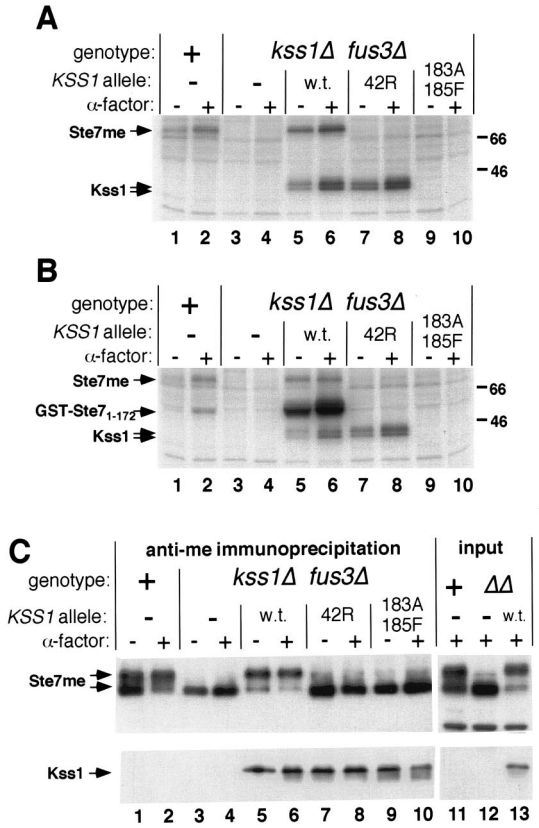

FIG. 6. Protein kinase activities of Ste7 and Kss1 in immune complexes. Cultures of strain YPH499 (*KSS1*$^+$ *FUS3*$^+$) or its isogenic derivative, YDM230 (*kss1*Δ *fus3*Δ), expressing Ste7me from a multicopy plasmid and coexpressing either an empty vector (−) or, from the same vector, normal Kss1 (w.t.), a catalytically inactive Kss1 mutant (42R), or an unactivatable Kss1 mutant (183A 185F), as indicated, were grown, treated or not treated with α-factor (as indicated), and harvested as described in Materials and Methods. Cell extracts were prepared and immunoprecipitated with anti-c-Myc MAb 9E10. The washed immune complexes were incubated with Mg^{2+} and [γ-^{32}P]ATP and either no exogenous substrate (A) or 0.5 μM GST-Ste7$_{1-172}$ for 4 min at 30°C (B) as described in Materials and Methods. Reaction products were resolved by SDS-PAGE on a 10% polyacrylamide gel, which was dried and analyzed by autoradiography. Migration positions of molecular mass markers are shown in kilodaltons on the right. (C) Samples of the reaction mixtures used for panel A were resolved by SDS-PAGE and analyzed by immunoblotting with anti-Ste7 (top panel) or anti-Kss1 (bottom panel) antiserum. Also, portions of the initial extracts (5% of the amount used for the immunoprecipitation reactions shown in lanes 2, 4, and 6) were analyzed in the same way (lanes 11 to 13).

been demonstrated before. To permit characterization of Kss1 activity in the absence of Fus3, immune complexes were collected from the *fus3*Δ *kss1*Δ double mutant in which Ste7me was expressed in combination with either the normal or a mutant version of Kss1 (Fig. 6A, lanes 5 to 10). Coexpression of native Kss1 markedly enhanced incorporation of label into Ste7me during the 4-min incubation (Fig. 6A, lanes 5 to 8), whereas no incorporation into Ste7me was observed when the cells coexpressed catalytically inactive (K42R) Kss1, demonstrating that Ste7me is a substrate of Kss1 in vitro. Under these conditions, a prominent doublet of bands with an apparent molecular mass of ~43 kDa was also generated during the reaction (Fig. 6A, lanes 5 to 8). These species have a mobility identical to that observed previously for Kss1 phosphorylated in vivo in a Ste7-dependent manner (59). Moreover, as seen previously in the whole-cell labeling experiments (59), incorporation into the ~43-kDa bands in vitro was enhanced in the immunoprecipitates from pheromone-treated cells (Fig. 6A, lanes 5 and 6). Likewise, as observed in vivo (59), incorporation into catalytically inactive Kss1 mutant in vitro was essentially as efficient as for normal Kss1 (Fig. 6A, lanes 7 and 8), whereas no incorporation into the unactivatable (T183A Y185F) Kss1 mutant was detectable (Fig. 6A, lanes 9 and 10). These results indicate (i) that Kss1 is a substrate for Ste7me in vitro (as well as vice versa) and (ii) that Ste7me phosphorylates Kss1 in vitro exclusively on Thr-183 and Tyr-185. On the basis of in vivo studies using site-directed mutants (59), it has been suggested that the upper band of the doublet represents Kss1 modified solely on Tyr-185, whereas the lower band represents Kss1 modified at both Thr-183 and Tyr-185.

To determine if the MAPKs in the coprecipitates were also capable of phosphorylating an exogenously added substrate, otherwise identical reactions were carried out in the presence of purified bacterially expressed GST-Ste7$_{1-172}$, a phosphoacceptor protein containing a cluster of six S/TP sites (as discussed above). As observed for phosphorylation of Ste7me, GST-Ste7$_{1-172}$ was phosphorylated by the activities present in the immune complexes isolated from wild-type cells or from cells expressing normal Kss1 (Fig. 6B, lanes 1, 2, 5, and 6). Compared with the incorporation observed with immunoprecipitates of unstimulated cells expressing Fus3 and Kss1 at endogenous levels (lane 1), phosphorylation of GST-Ste7$_{1-172}$ was increased approximately 3-fold when the immunoprecipitates were isolated from pheromone-treated cells (lane 2) and was stimulated at least 10-fold when Kss1 was overproduced (lane 5) and as much as 30-fold when the Kss1-overproducing cells were stimulated with α-factor (lane 6). Phosphorylation of GST-Ste7$_{1-172}$ (and Ste7me) did not occur in reactions that lacked Kss1 or Fus3 (lanes 3 and 4) or in reactions that contained only catalytically inactive Kss1 (lanes 7 and 8) or unactivatable Kss1 (lanes 9 and 10). As revealed by immunoblotting (Fig. 6C), both the normal and mutant forms of Kss1 coimmunoprecipitated with Ste7me to approximately the same degree from both naive and pheromone-stimulated cells. Kss1 and Fus3 expressed at their endogenous levels were readily detectable in the coprecipitates with overproduced Ste7me by virtue of their kinase activities (Fig. 6A and B, lanes 1 and 2) but were more difficult to detect reliably by immunoblot analysis (Fig. 6C, lanes 1 and 2, and data not shown).

GST itself was not a substrate (data not shown) in these reactions, nor was BSA, which was present in the assay buffer at a concentration of 15 μM (see Materials and Methods). However, myelin basic protein (MBP), a known substrate of many MAPKs (29, 32), was an exogenous substrate for Kss1 under these conditions (see below); but to achieve a comparable degree of incorporation, a higher concentration of MBP (25 μM) than of GST-Ste7$_{1-172}$ (0.5 μM) was required. Results similar to those described above were obtained when Fus3 was overproduced with Ste7me (instead of Kss1) in the *fus3*Δ *kss1*Δ strain; the Ste7me-Fus3 immune complexes catalyzed phosphorylation of GST-Ste7$_{1-172}$ (and Ste7me) and MBP (but not GST or BSA), and incorporation was enhanced when the cells were pretreated with pheromone (data not shown).

The Ste7-Kss1 complex is not an enzyme-substrate complex. The preceding results indicated that in the isolated complexes, Ste7 was able to phosphorylate Kss1, and Kss1 was able to phosphorylate Ste7. However, the experiments did not establish whether both phosphorylation reactions could occur while both proteins remained bound in the complex or whether prior dissociation and rebinding were required to permit one or the other phosphorylation reaction (or both reactions) to occur (Fig. 7A). The fact that GST-Ste7$_{1-172}$ not only contains six S/TP sites for phosphorylation by Kss1 but also harbors the

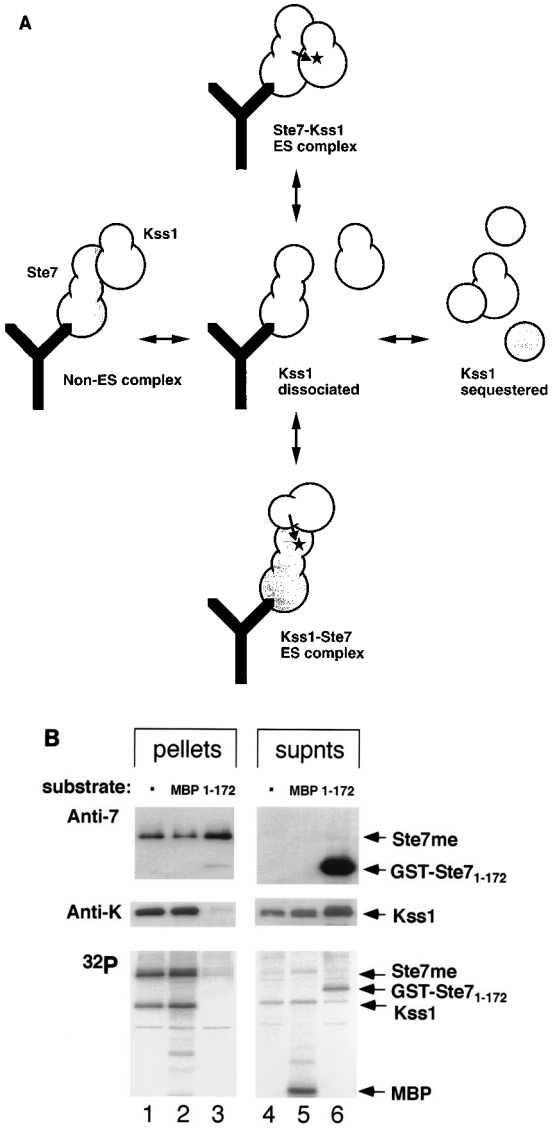

FIG. 7. Dynamics of Ste7-Kss1 interaction and mutual phosphorylation. (A) Depicted schematically are the transitions between the various possible complexes between Ste7 and Kss1 that can presumably occur during the immune complex kinase assay (see the legend to Fig. 6) and the substrate capture experiment performed as described for panel B. Ste7me, with its N-terminal extension and two-domain catalytic core, shown as a three-lobed molecule (shaded spheres), is bound by anti-c-Myc MAb 9E10 (Y), which recognizes the epitope fused to the C terminus of Ste7. Kss1, with its two-domain catalytic core, shown as a two-lobed molecule (open spheres), can associate with Ste7 in a non-ES complex (left), as a Ste7-Kss1 ES complex poised to permit phosphorylation (star) of Kss1 (top), or as a Kss1-Ste7 ES complex poised to permit phosphorylation (star) of Ste7 (bottom). In the presence (right) of excess GST-$Ste7_{1-172}$ (shaded circle), any Kss1 released into solution will be sequestered and prevented from rebinding to Ste7 in any mode. (B) To prepare complexes of activated Ste7me bound to unactivated Kss1, a cell extract prepared from strain E929-6C-1 (*ste7*Δ), overproducing Kss1 and not treated with pheromone, was mixed with an equal mass of protein from an extract prepared from strain YDM230 (*kss1*Δ *fus3*Δ), overproducing Ste7me and treated with α-factor, and immunoprecipitated with anti-c-Myc MAb 9E10. Suspensions of the washed complexes were divided into three equal portions and incubated for 4 min at 30°C with Mg^{2+} and [γ-^{32}P]ATP and with either no exogenous substrate (lanes 1 and 4), 50 μM MBP (lanes 2 and 5), or 5 μM GST-$Ste7_{1-172}$ (lanes 3 and 6). After quenching, the reactions were separated into the material still bound to the MAb-protein A/G beads (pellets; lanes 1 to 3) and the material in the corresponding supernatant fractions (supnts; lanes 4 to 6) as described in Materials and Methods. These fractions were then solubilized and divided into three equal portions, which were resolved by SDS-PAGE on three separate gels and either dried and analyzed by autoradiography (^{32}P) or analyzed by immunoblotting with either anti-Ste7 (Anti-7) or anti-Kss1 (Anti-K) antisera.

domain responsible for high-affinity binding of Ste7 (Fig. 2) suggested an experimental method for addressing the nature of the Ste7-Kss1 complex isolated by immunoprecipitation. We reasoned that by adding an excess of GST-$Ste7_{1-172}$ to the immune complexes just prior to initiating the kinase reaction, any Kss1 that dissociated into solution would be trapped as Kss1-GST-$Ste7_{1-172}$ complexes. If phosphorylation of Kss1 by Ste7 (or vice versa) occurs directly in the complex, these reactions would not be impeded by the presence of the exogenous competitor (given the reasonable assumption that k_{cat} is greater than k_{off}). However, if phosphorylation of Kss1 by Ste7 (or vice versa) proceeds through an intermediate step in which Kss1 dissociates into solution, the capture of Kss1 by GST-$Ste7_{1-172}$ would prevent its phosphorylation by Ste7 and/or its phosphorylation of Ste7 (Fig. 7A). A phosphoacceptor substrate for Kss1 that lacks a high-affinity binding site would not effectively capture Kss1. This approach is similar to the template challenge method used to determine whether a polynucleotide-tracking enzyme is processive or distributive (54).

To ensure that such reactions were conducted with immune complexes that initially contained only unactivated Kss1, an extract was prepared from a *fus3*Δ *kss1*Δ mutant that overproduced Ste7me protein and was treated with α-factor, which was mixed with an extract prepared from a *ste7*Δ strain that overproduced Kss1. Bead-bound immune complexes containing activated Ste7me and unactivated Kss1 were isolated from the resulting mixture and apportioned into three equal aliquots. To initiate the kinase reaction, each sample received [γ-^{32}P]ATP · Mg^{2+} and either no exogenous protein, 5 μM GST-$Ste7_{1-172}$, or, as a control, 50 μM MBP. After 4 min at 30°C, each suspension was separated into a pellet and supernatant fraction, which were analyzed separately (Fig. 7B).

Ste7me remained bound to the antibody on the beads throughout the course of the reaction, as expected (Fig. 7B, upper panels). As anticipated from the half-time for dissociation of the Ste7-Kss1 complex at 30°C, a substantial fraction of the Kss1 dissociated into the soluble fraction during the course of the incubation (Fig. 7B, middle panels). In the absence of any exogenous protein or when MBP was present, the majority of the Kss1 was able to rebind to the Ste7me on the beads, whereas when GST-$Ste7_{1-172}$ was present nearly all of the Kss1 remained in the supernatant solution, indicating that GST-$Ste7_{1-172}$ did effectively sequester the released Kss1. Most significantly, in the presence of GST-$Ste7_{1-172}$, incorporation of label into both Ste7me and Kss1 was completely blocked, whereas in its absence or in the presence of MBP, prominent phosphorylations of both Kss1 and Ste7me were observed. Moreover, although GST-$Ste7_{1-172}$ is an excellent substrate for activated Kss1 (Fig. 6B), only a very modest degree of incorporation into GST-$Ste7_{1-172}$ was detected under these conditions, indicating that the Kss1 released from the Ste7-Kss1 complex and captured by the GST-$Ste7_{1-172}$ was primarily in the unactivated form, as expected. In the absence of competitor, Ste7me, Kss1, and, when added, MBP became prominently labeled, indicating that the released Kss1 had become phosphorylated and activated by Ste7. These results suggest that the initial high-affinity Ste7-Kss1 complex isolated from cells by immunoprecipitation must dissociate before either Kss1 or Ste7 can be phosphorylated. Thus, the initial high-affinity complex appears to be neither a Ste7-Kss1 ES complex nor a Kss1-Ste7 ES complex.

In assays in which complexes containing both activated Kss1 and Ste7me, or activated Kss1 bound to unactivated Ste7me, were used, phosphorylation of Ste7me in the pellet was inhibited by the presence of GST-$Ste7_{1-172}$ in solution (data not shown), confirming that to phosphorylate Ste7me, activated

TABLE 2. Reduction of mating efficiency by deletion of the Kss1- and Fus3-binding site of Ste7

Strain	Plasmid	Ste7 derivative	Expt 1		Expt 2	
			Mating efficiency[a]	Relative mating efficiency[b]	Mating efficiency	Relative mating efficiency
E929-6C(*STE*$^+$)	YCplac22	Ste7	0.27	1.00	0.65	1.00
E929-6C-1(*ste7*Δ)	YCplac22	None	$<2 \times 10^{-7}$	$<8 \times 10^{-7}$	$<2 \times 10^{-7}$	$<4 \times 10^{-7}$
	YCpT-*STE7*	Ste7	0.22	0.81	0.51	0.78
	YCpT-*STE7(171-515)*	$Ste7_{171–515}$	0.04	0.16	0.04	0.06
	YCpT-*STE7(23-515)*	$Ste7_{23–515}$	ND[c]	ND	0.05	0.07

[a] Crossed with strain DC17 (Table 1).
[b] Relative to strain E929-6C(*STE*$^+$) carrying plasmid YCplac22.
[c] ND, not determined.

Kss1 has to first dissociate from the high-affinity complex into solution. When an essentially identical procedure was used to examine the nature of the high-affinity Ste7-Fus3 complex isolated from cell extracts by immunoprecipitation, very similar results were obtained (data not shown). Hence, the Ste7-Fus3 complex also is, most likely, neither a Ste7-Fus3 ES complex nor a Fus3-Ste7 ES complex.

The domain of Ste7 required for tight binding of Kss1 and Fus3 is necessary for optimal pheromone response. To determine if the strong interaction observed between Ste7 and Kss1 (and Fus3) produced in vitro and in cell extracts has a discernible role in pheromone response in vivo, two mutant alleles of *STE7*, *STE7(23-515)* and *STE7(171-515)*, were constructed. These alleles leave the catalytic core completely intact but remove 21 residues (codons 2 to 22) and 169 residues (codons 2 to 170), respectively, of the *STE7* coding sequence, which corresponds to the segment of the N-terminal domain of Ste7 that we demonstrated was required for its high-affinity binding of Kss1 and Fus3 in vitro (Fig. 2). It has been shown previously that deletion of the N terminus of Ste7 does not eliminate its ability to bind to Ste5 (17, 72) or its ability to be phosphorylated and activated by Ste11 (66). To examine the effects of these alterations on the mating response, either the normal *STE7* gene or each of the two N-terminally truncated mutant genes was expressed under the control of the endogenous *STE7* promoter on a low-copy-number (*CEN*) plasmid in a *MAT***a** *ste7*Δ strain. These cells were then subjected to three different tests of pheromone response.

First, as a measure of the short-term effects of pheromone action, a plasmid carrying a *PRE-lacZ* construct was introduced into the same strains, and the level of induction of this Ste12-dependent reporter gene by α-factor treatment of the cells was examined. Compared with the *ste7*Δ strain expressing the wild-type *STE7* gene from the *CEN* plasmid, cells expressing the *STE7(171-515)* allele from the same plasmid exhibited a 7- to 10-fold reduction in the level of β-galactosidase produced after 1 h of pheromone treatment (data not shown). The *STE7(23-515)* allele was not tested. Second, as a measure of the long-term effects of pheromone action, pheromone-induced G_1 arrest and recovery from arrest were monitored in the standard halo bioassay (75). Compared with normal cells or the *ste7*Δ strain expressing the wild-type *STE7* gene from the *CEN* plasmid, cells expressing either the *STE7(23-515)* or the *STE7(171-515)* allele from the *CEN* plasmid were less sensitive to pheromone-imposed cell cycle arrest, as judged by a reduction in initial halo diameter (data not shown). More strikingly, however, recovery from pheromone-imposed G_1 arrest was much more rapid, as judged by the rate of development of turbidity in the halos, for the cells expressing either the *STE7(23-515)* or the *STE7(171-515)* allele than for cells expressing the wild-type *STE7* gene (data not shown). Even when the *MAT***a** *ste7*Δ strain expressed the *STE7(171-515)* allele from the strong *GAL1* promoter, the cells exhibited comparable defects in pheromone response, suggesting that the phenotype of this allele was not due to a decreased level of expression or to a decrease in stability of the mutant protein (data not shown). We also confirmed by immunoblotting that Ste7 and $Ste7_{23–515}$ proteins were produced at comparable levels and had comparable stabilities (data not shown).

Third, and most significantly, as a measure of overall mating proficiency, we performed quantitative mating assays (Table 2). When transformed with the *CEN* vector alone, the *ste7*Δ strain was completely sterile in a quantitative mating assay (frequency of diploid formation, $<2 \times 10^{-7}$), whereas expression of the wild-type *STE7* gene inserted into the same vector restored mating to close to the level seen for an otherwise isogenic strain carrying an intact *STE7*$^+$ gene on the chromosome (Table 2). Compared with cells expressing *STE7*, however, cells expressing either *STE7(23-515)* or *STE7(171-515)* reproducibly exhibited a 5- to 17-fold reduction in the frequency of diploid formation (Table 2).

In summary, by every measure tested, the loss of the domain of Ste7 required for its tight binding to Kss1 and Fus3 in vitro substantially reduced (approximately 10-fold) the efficiency of the mating response in vivo. While these defects were readily evident, it is clear that both mutant alleles retained a significant level of residual function, relative to a *ste7*Δ null allele (Table 2).

DISCUSSION

A stable MEK-MAPK complex. Phosphorylation and activation of a MAPK by its upstream MEK is a crucial step for signal transmission in signaling pathways that involve a MAPK cascade. In this study, we used the MAPKs (Kss1 and Fus3) and the MEK (Ste7) of the *S. cerevisiae* pheromone response pathway to demonstrate that these enzymes form a specific, high-affinity (K_d of ~5 nM), and relatively stable (half-time for dissociation of ~2 min at 30°C) complex with each other. To our knowledge, this interaction is the tightest and the most thoroughly characterized for any MAPK and MEK described for any organism. In addition, in the course of these studies, we have shown for the first time that Ste7 can phosphorylate and activate Kss1 in vitro and that once phosphorylated and activated, Kss1 has protein phosphotransferase activity in vitro. Moreover, we have demonstrated that the N terminus of Ste7 is a substrate for both Kss1 and Fus3; hence, Kss1- and Fus3-dependent modifications in this region may be of physiological significance for the activity, stability, and/or localization of Ste7 in vivo.

Despite the fact that Ste7, Kss1, and Fus3 are all protein kinases and, as we demonstrated, capable of phosphorylating each other, we found, somewhat surprisingly perhaps, that the known or putative phosphoacceptor sites for these reactions on each protein were not required for the formation of the high-affinity Ste7-Kss1 or Ste7-Fus3 complexes. In agreement with this observation, we found that the stability of the Ste7-Kss1 and Ste7-Fus3 complexes was not markedly affected by the phosphorylation state of either partner. Using an enzyme capture approach, we confirmed that the stable Ste7-MAPK complex isolated from cell extracts is not an ES complex. Finally, we showed that mutations in Ste7 that eliminate its high-affinity binding site for Kss1 and Fus3 reduce signal output in the pheromone response pathway to 10% of its normal level. Our findings have important implications both for signal propagation in the pheromone response pathway and for the role of protein-protein interactions in signal transduction pathways generally.

Specificity and generality of the stable MEK-MAPK complex. Both *S. cerevisiae* and a mammalian cell contain parallel MAPK cascades that transmit different signals (16, 42, 68). How such parallel pathways are insulated from each other is an important and largely unexplored issue (5). In this context, the specificity of the complex between Ste7 and Kss1 (or Fus3) is noteworthy; Ste7 did not detectably associate in vitro with two other MAPKs that are present in haploid yeast cells (Hog1 and Mpk1) or with a mammalian MAPK (Erk2). From estimates of the number of molecules of Kss1 (~5,000), Fus3 (~5,000), and Ste7 (<2,000) per cell, obtained from quantitative immunoblotting of extracts with known amounts of the in vitro translation products to prepare standard curves (4b), and from the K_d of 5 nM, it can be calculated that >95% of the Ste7 molecules in an unstimulated haploid should be bound to Kss1 and/or Fus3 at any given instant. This situation would further decrease the probability that Ste7 could interact, even transiently, with other MAPKs. Likewise, neither Kss1 nor Fus3 (epitope tagged) was able to bind detectably to Pbs2 (the MEK for Hog1). Taken together, these findings suggest that parallel MAPK cascades may be insulated from each other, in part, by formation of relatively stable complexes between the MEK and the MAPK components within the same pathway.

Using coimmunoprecipitation of radiolabeled proteins synthesized in vitro, we were unable to detect interaction between Pbs2 and Hog1 (epitope tagged) or between mammalian MEK1 and Erk2 (4a). However, this assay method cannot reliably detect interactions that have a K_d above 0.5 to 1 μM or any associations that have a half-time for dissociation of <1 min at 4°C (because these would be lost during the wash steps used in our procedure). On the other hand, in studies using the less quantitative but potentially more sensitive two-hybrid approach in vivo and/or affinity chromatography in vitro (71), interactions between mammalian MEKs and ERKs (98) and between the MAPK (Mpk1) of the yeast *PKC1* pathway and its MEKs (Mkk1 and Mkk2) (83) have been found. Likewise, interaction between Ste7 and Fus3, and between Ste7 and Kss1, has also been detected by two-hybrid analysis (17, 60, 72). Thus, strong MEK-MAPK association is likely to be a common feature of many MAPK signaling modules, although the interactions between Kss1 or Fus3 and Ste7 seem exceptionally stable.

Function of the complex. Because deletion of the sequences in Ste7 required for its high-affinity binding to Kss1 and Fus3 in vitro caused readily detectable reductions in vivo in pheromone-induced transcription, in pheromone-imposed cell cycle arrest, and in the frequency of diploid formation, it appears that tight association of Ste7 with Kss1 and Fus3 allows for more efficient signal transmission and amplification at the MAPK activation step of the pathway.

Contrary to the prevailing view of protein kinase-substrate specificity as being mediated predominantly by interactions between the catalytic cleft of the enzyme and a contiguous stretch of residues immediately surrounding the phosphoacceptor site in the substrate (51–53), we have demonstrated here that formation of a very specific and very high affinity complex between a protein kinase (Ste7) and its substrate (Kss1) can occur without the participation of either its catalytic domain or the phosphoacceptor sites on its substrate. One role of such a strong and selective interaction may be to impart a second layer of specificity on top of that provided by recognition of the target phosphoacceptor sequence by the active site. In this way, proper activation of a MAPK by its upstream MEK would involve a double selection. A similar mechanism has been suggested as a means by which protein-tyrosine kinases recruit the correct SH2 domain-containing substrates to ensure specificity and fidelity in growth factor-initiated signaling pathways (20, 27, 63, 67, 85). Another role for the high-affinity complex may simply be to raise the local effective concentration of the MEK as an additional means to ensure efficient MAPK activation or to raise the local concentration of the MAPK to ensure efficient feedback modulation of its MEK, or both. A similar suggestion has been made recently to explain the purpose of the tight binding, demonstrated by affinity chromatography, between a MAPK, Jnk, and one of its cellular substrates, the c-Jun transcription factor (49). Yet another potential function for such a tight complex between a MEK and its target MAPK may be to ensure effective mutual intracellular targeting and colocalization of the proteins in the cell.

Structural basis of the complex. The high-affinity binding of Ste7 and Kss1, and of Ste7 and Fus3, provides a useful paradigm for a novel class of protein kinase-target interactions. Kss1 is a substrate of Ste7, and Ste7 is a substrate of Kss1, as demonstrated by the biochemical results presented here. Likewise, Ste7 phosphorylates Fus3, and Fus3 phosphorylates Ste7, as shown by others (33) and confirmed here. If a protein kinase associates strongly with a substrate, there are two possibilities to explain the structural basis of such a stable interaction: (i) the majority of the binding energy is contributed by contacts between the catalytic pocket of the enzyme and residues surrounding the phosphoacceptor site in the substrate (a typical ES complex); and (ii) the majority of the binding energy is supplied by contacts between residues elsewhere on the surfaces of the two proteins. While the second alternative appears to be the case for the Ste7-Kss1 and Ste7-Fus3 interactions, it is nonetheless possible that in the complex, one or the other enzyme (or both) is positioned as an ES complex and thus poised to phosphorylate its target sequence. Our results, however (Fig. 7), suggest that the stable high-affinity complexes between Ste7 and its MAPKs appear to correspond to the non-ES complex depicted in Fig. 7A. The existence of this complex presumably increases the probability that subsequent (and more transient) ES complexes can be formed, leading to greater efficiency in the phosphorylation and activation of the MAPKs and in the phosphorylation and modulation of the MEK. For example, when Ste7 and Kss1 are bound in the high-affinity complex, access of other proteins to the catalytic pocket of Ste7 may be blocked. At the instant the high-affinity complex dissociates, the catalytic pocket of Ste7 is empty and Kss1 is the closest available protein. Once activated, Kss1 can phosphorylate the nearby Ste7. In this way, the double selection provided by tightly binding MEK-MAPK interactions that are separate from active site recognition of phosphoacceptor sites can operate in two kinetically distinct steps.

It is possible that the transition from the high-affinity complex to ES complexes involves a conformational change rather than dissociation. However, since formation of ES complexes was blocked by the presence of competing MAPK binding sites in solution, any such conformational change mechanism must have properties similar to those of the simpler dissociation model that we favor. Yet another possibility to explain our results is that in the high-affinity complex, Ste7 and Kss1 are situated in an enzyme-substrate orientation, but the active site is not accessible to the exogenously added ATP. Dissociation of the high-affinity complex would then be required to detect any incorporation of label. Nevertheless, since MAPK activation requires two phosphorylation events, dissociation of the high-affinity MEK-MAPK complex must obligatorily precede the dual phosphorylation of the MAPK.

Extensions to other protein kinase interactions. In the cell, Ste7-Kss1 and Ste7-Fus3 complexes will be influenced by association of Ste7, Kss1, and Fus3 with other proteins. In particular, all three enzymes appear to interact with Ste5 protein (17, 60, 72), prompting proposals (30, 79) that one of the functions of Ste5 is to serve as a scaffold or platform that is required to bring the components of the MAPK cascade into contact with one another. We have clearly shown here, however, that the tight binding of Ste7 to Kss1 or Fus3 is direct and does not require the presence of Ste5 in vitro or in cell extracts. Other results also suggest a considerable degree of independence of the MAPK cascade from Ste5. Ste11 can phosphorylate and activate Ste7 in vitro, which, in turn, can phosphorylate Fus3, all in the absence of Ste5 (66). Also, dominant constitutively active alleles of *STE11* can bypass the requirement for *STE5* in vivo (14, 88). Finally, Ste20, Ste11, Ste7, and probably Kss1 are involved in the haploid invasive growth pathway and the diploid pseudohyphal growth pathway, whereas Ste5 is not (58, 77). Thus, we believe that the sterility of *ste5* null strains is due to a defect at or upstream of the level of Ste11 and that the proposed platform function of Ste5 is ancillary. The interaction of Ste5 with Ste7 and Kss1/Fus3 may have a function similar to (and perhaps partially redundant with) that of the direct Ste7-Kss1/Fus3 interaction characterized here. Association of Ste11, Ste7, Kss1, and Fus3 with Ste5 may increase their local effective concentrations, thereby enhancing the rate of signal transmission and providing an additional layer of specificity that insulates the MAPKs of the pheromone signaling cascade from other signaling pathways (96).

To distinguish between the myriad of possible functions for the interaction of Ste5 with the members of the associated MAPK cascade, it will be important to determine whether binding of any of these components to Ste5 positions any of the enzymes in an ES complex (either with each other or with Ste5). The experimental strategy developed in this study could be applied to this question. Furthermore, this same strategy could be adapted to explore the nature of other putative protein kinase-scaffold interactions (20, 46, 63, 67), other protein kinase-substrate interactions (49, 50, 74), and other protein kinase-protein kinase associations (44, 45, 93, 98).

The high-affinity MEK-MAPK interaction characterized here represents a single link in a network of noncatalytic protein-protein interactions between the members of a multicomponent signal transduction pathway. The significant effects of the disruption of this single link suggests that the network of such links, collectively, substantially influences signaling dynamics.

ACKNOWLEDGMENTS

We thank George Boguslawski, Melanie Cobb, Beverly Errede, Stanley Fields, Gerald Fink, Michael Gustin, George F. Sprague, Jr., and George Yancopoulos, and especially Carla Inouye and Doreen Ma of our laboratory, for gifts of reagents.

This work was supported by NIH-NRSA postdoctoral fellowship GM15871 (to L.B.); by NIH predoctoral traineeship GM07232 and an Academic Development Program predoctoral fellowship from Merck & Co., Inc. (to J.G.C.); by an American Society for Microbiology undergraduate summer research fellowship and a University of California President's Undergraduate Research Fellowship (to E.C.C.); and by facilities provided by the Berkeley campus Cancer Research Laboratory and by NIH research grant GM21841 (to J.T.).

REFERENCES

1. **Ahn, N. G., R. Seger, and E. G. Krebs.** 1992. The mitogen-activated protein kinase activator. Curr. Opin. Cell Biol. **4:**992–999.
2. **Ammerer, G.** 1993. Sex, stress and integrity: the importance of MAP kinases in yeast. Curr. Opin. Genet. Dev. **4:**90–95.
3. **Avruch, J., X. Zhang, and J. M. Kyriakis.** 1994. Raf meets ras: completing the framework of a signal transduction pathway. Trends. Biochem. Sci. **19:**279–283.
4. **Bardwell, A. J., L. Bardwell, N. Iyer, J. Q. Svejstrup, W. J. Feaver, R. D. Kornberg, and E. C. Friedberg.** 1994. Yeast nucleotide excision repair proteins Rad2 and Rad4 interact with RNA polymerase II basal transcription factor b (TFIIH). Mol. Cell. Biol. **14:**3569–3576.

4a. **Bardwell, L.** Unpublished results.

4b. **Bardwell, L., and E. C. Chang.** Unpublished results.

5. **Bardwell, L., J. G. Cook, C. J. Inouye, and J. Thorner.** 1994. Signal propagation and regulation in the mating pheromone response pathway of the yeast *Saccharomyces cerevisiae*. Dev. Biol. **166:**363–379.
6. **Bardwell, L., A. J. Cooper, and E. C. Friedberg.** 1992. Stable and specific association between the yeast recombination and DNA repair proteins RAD1 and RAD10 in vitro. Mol. Cell. Biol. **12:**3041–3049.
7. **Bax, B., and H. Jhoti.** 1995. Protein-protein interactions: putting the pieces together. Curr. Biol. **5:**1119–1121.
8. **Blumer, K. J., and G. L. Johnson.** 1994. Diversity in function and regulation of MAP kinase pathways. Trends Biochem. Sci. **19:**236–240.
9. **Boeke, J. D., J. Trueheart, G. Natsoulis, and G. R. Fink.** 1987. 5′-Fluoroorotic acid as a selective agent in yeast molecular genetics. Methods Enzymol. **152:**164–175.
10. **Boguslawski, G.** 1992. *PBS2*, a yeast gene encoding a putative protein kinase, interacts with the *RAS2* pathway and affects the osmotic sensitivity of *Saccharomyces cerevisiae*. J. Gen. Microbiol. **138:**2425–2432.
11. **Boulton, T. G., et al.** 1991. ERKs: a family of protein-serine/threonine kinases that are activated and tyrosine phosphorylated in response to insulin and NGF. Cell **65:**663–675.
12. **Brewster, J. L., T. De Valoir, N. D. Dwyer, E. Winter, and M. C. Gustin.** 1993. An osmosensing signal transduction pathway in yeast. Science **259:**1760–1763.
13. **Brill, J. A., E. A. Elion, and G. R. Fink.** 1994. A role for autophosphorylation revealed by activated alleles of FUS3, the yeast MAP kinase homolog. Mol. Biol. Cell **5:**297–312.
14. **Cairns, B. R., S. W. Ramer, and R. D. Kornberg.** 1992. Order of action of components in the yeast pheromone response pathway revealed with a dominant allele of the STE11 kinase and the multiple phosphorylation of the STE7 kinase. Genes Dev. **6:**1305–1318.
15. **Campbell, J. S., R. Seger, J. D. Graves, L. M. Graves, A. M. Jensen, and E. G. Krebs.** 1995. The MAP kinase cascade. Recent Prog. Hormone Res. **50:**131–159.
16. **Cano, E., and L. C. Mahadevan.** 1995. Parallel signal processing among mammalian MAPKs. Trends Biochem. Sci. **20:**117–122.

16a. **Chang, E. C., and B. R. Cairns.** Unpublished results.

17. **Choi, K.-Y., B. Satterberg, D. M. Lyons, and E. A. Elion.** 1994. Ste5 tethers multiple protein kinases in the MAP kinase cascade required for mating in S. cerevisiae. Cell **78:**499–512.
18. **Ciejek, E. M., and J. Thorner.** 1979. Recovery of *S. cerevisiae* **a** cells from G1 arrest by alpha-factor pheromone requires endopeptidase action. Cell **18:**623–635.
19. **Cobb, M. H., and E. J. Goldsmith.** 1995. How MAP kinases are regulated. J. Biol. Chem. **270:**14843–14846.
20. **Cohen, G. B., R. Ren, and D. Baltimore.** 1995. Modular binding domains in signal transduction proteins. Cell **80:**237–248.
21. **Company, M., C. Adler, and B. Errede.** 1988. Identification of a Ty1 regulatory sequence responsive to STE7 and STE12. Mol. Cell. Biol. **8:**2545–2554.
22. **Courchesne, W. E., R. Kunisawa, and J. Thorner.** 1989. A putative protein kinase overcomes pheromone-induced arrest of cell cycling in *S. cerevisiae*. Cell **58:**1107–1119.
23. **Davis, J. L., R. Kunisawa, and J. Thorner.** 1992. A presumptive helicase

(*MOT1* gene product) affects gene expression and is required for viability in the yeast *Saccharomyces cerevisiae*. Mol. Cell. Biol. **12:**1879–1892.
24. **Davis, R. J.** 1993. The mitogen-activated protein kinase signal transduction pathway. J. Biol. Chem. **268:**14553–14556.
25. **Davis, R. J.** 1994. MAPKs: new JNK expands the group. Trends Biochem. Sci. **19:**470–473.
26. **Deutscher, M. P. (ed.).** 1990. Methods in Enzymology, vol. 182. Guide to protein purification. Academic Press, San Diego, Calif.
27. **Duyster, J., R. Baskaran, and J. Y. Wang.** 1995. Src homology 2 domain as a specificity determinant in the c-Abl-mediated tyrosine phosphorylation of the RNA polymerase II carboxyl-terminal repeated domain. Proc. Natl. Acad. Sci. USA **92:**1555–1559.
28. **Elion, E., P. Grisafi, and G. Fink.** 1990. FUS3 encodes a cdc2+/CDC28-related kinase required for the transition from mitosis into conjugation. Cell **60:**649–664.
29. **Elion, E., B. Satterberg, and J. Kranz.** 1993. Fus3 phosphorylates multiple components of the mating signal transduction cascade: evidence for Ste12 and Far1. Mol. Biol. Cell **4:**495–510.
30. **Elion, E. A.** 1995. Ste5: a meeting place for MAP kinases and their associates. Trends Cell Biol. **5:**322–327.
31. **Elion, E. A., J. A. Brill, and G. R. Fink.** 1991. FUS3 represses CLN1 and CLN2 and in concert with KSS1 promotes signal transduction. Proc. Natl. Acad. Sci. USA **88:**9392–9396.
32. **Erickson, A. K., D. M. Payne, P. A. Martino, A. J. Rossomando, J. Shabanowitz, M. J. Weber, D. F. Hunt, and T. W. Sturgill.** 1990. Identification by mass spectrometry of threonine 97 in bovine myelin basic protein as a specific phosphorylation site for mitogen-activated protein kinase. J. Biol. Chem. **265:**19728–19735.
33. **Errede, B., A. Gartner, Z. Zhou, K. Nasmyth, and G. Ammerer.** 1993. MAP kinase-related FUS3 from *S. cerevisiae* is activated by STE7 *in vitro*. Nature (London) **362:**261–264.
34. **Evan, G. I., G. K. Lewis, G. Ramsay, and J. M. Bishop.** 1985. Isolation of monoclonal antibodies specific for human c-*myc* proto-oncogene product. Mol. Cell. Biol. **5:**3610–3616.
35. **Gartner, A., K. Nasmyth, and G. Ammerer.** 1992. Signal transduction in *Saccharomyces cerevisiae* requires tyrosine and threonine phosphorylation of FUS3 and KSS1. Genes Dev. **6:**1280–1292.
36. **Gietz, D., A. St. Jean, R. A. Woods, and R. H. Schiestl.** 1992. Improved method for high efficiency transformation of intact yeast cells. Nucleic Acids Res. **20:**1425.
37. **Gietz, R. D., and A. Sugino.** 1988. New yeast-*Escherichia coli* shuttle vectors constructed with in vitro mutagenized yeast genes lacking six-base pair restriction sites. Gene **74:**527–534.
38. **Hanks, S. K., and T. Hunter.** 1995. Protein kinases 6. The eukaryotic protein kinase superfamily: kinase (catalytic) domain structure and classification. FASEB J. **9:**576–596.
39. **Harlow, E., and D. Lane.** 1988. Antibodies: a laboratory manual. Cold Spring Harbor Laboratory Press, Cold Spring Harbor, N.Y.
40. **Hasson, M. S., D. Blinder, J. Thorner, and D. D. Jenness.** 1994. Mutational activation of the *STE5* gene product bypasses the requirement for G protein β and γ subunits in the yeast pheromone response pathway. Mol. Cell. Biol. **14:**1054–1065.
41. **Herskowitz, I.** 1995. MAP kinase pathways in yeast: for mating and more. Cell **80:**187–197.
42. **Hill, C. S., and R. Treisman.** 1995. Transcriptional regulation by extracellular signals: mechanisms and specificity. Cell **80:**199–211.
43. **Hill, J. E., A. M. Myers, T. J. Koerner, and A. Tzagoloff.** 1986. Yeast/*E. coli* shuttle vectors. Yeast **2:**163–167.
44. **Hsiao, K.-M., S.-Y. Chou, S.-J. Shih, and J. E. Ferrell, Jr.** 1994. Evidence that inactive p42 mitogen-activated protein kinase and inactive Rsk exist as a heterodimer *in vivo*. Proc. Natl. Acad. Sci. USA **91:**5480–5484.
45. **Huang, W., A. Alessandrini, C. M. Crews, and R. L. Erikson.** 1993. RAF-1 forms a stable complex with MEK1 and activates MEK1 by serine phosphorylation. Proc. Natl. Acad. Sci. USA **90:**10947–10951.
45a. **Inouye, C. J., and J. Thorner.** Unpublished results.
46. **Jones, D. H., S. Ley, and A. Aitken.** 1995. Isoforms of 14-3-3 protein can form homo- and heterodimers *in vivo* and *in vitro*: implications for function as adaptor proteins. FEBS Lett. **368:**55–58.
47. **Jones, E. W.** 1991. Tackling the protease problem in yeast. Methods Enzymol. **194:**428–453.
48. **Julius, D., L. Blair, A. Brake, G. Sprague, and J. Thorner.** 1983. Yeast α-factor precursor is processed from a larger precursor polypeptide: the essential role of a membrane-bound dipeptidyl aminopeptidase. Cell **32:**839–852.
49. **Kallunki, T., B. Su, I. Tsigelny, H. K. Sluss, B. Dérijard, G. Moore, R. Davis, and M. Karin.** 1994. JNK2 contains a specificity-determining region responsible for efficient c-Jun binding and phosphorylation. Genes Dev. **8:**2996–3007.
50. **Karin, M.** 1994. Signal transduction from the cell surface to the nucleus through the phosphorylation of transcription factors. Curr. Opin. Cell Biol. **6:**415–424.
51. **Kemp, B. E., M. W. Parker, S. Hu, T. Tiganis, and C. House.** 1994. Substrate and pseudeosubstrate interactions with protein kinases: determinants of specificity. Trends Biochem. Sci. **19:**440–444.
52. **Kemp, B. E., and R. B. Pearson.** 1990. Protein kinase recognition sequence motifs. Trends Biochem. Sci. **200:**342–346.
53. **Kennelly, P. J., and E. G. Krebs.** 1991. Consensus sequences as substrate specificity determinants for protein kinases and protein phosphatases. J. Biol. Chem. **266:**15555–15558.
54. **Kornberg, A., and T. A. Baker.** 1995. DNA replication. W. H. Freeman, New York.
55. **Kurjan, J.** 1993. The pheromone response pathway in *Saccharomyces cerevisiae*. Annu. Rev. Genet. **27:**147–179.
56. **Lee, K. S., K. Irie, Y. Gotoh, Y. Watanabe, H. Araki, E. Nishida, K. Matsumoto, and D. E. Levin.** 1993. A yeast mitogen-activated protein kinase homolog (Mpk1p) mediates signalling by protein kinase C. Mol. Cell. Biol. **13:**3067–3075.
57. **Levin, D. E., and B. Errede.** 1995. The proliferation of MAP kinase signaling pathways in yeast. Curr. Opin. Cell Biol. **7:**197–202.
58. **Liu, H., C. Styles, and G. R. Fink.** 1993. Elements of the yeast pheromone response pathway required for filamentous growth of diploids. Science **262:**1741.
59. **Ma, D., J. G. Cook, and J. Thorner.** 1995. Phosphorylation and localization of Kss1, a MAP kinase of the *Saccharomyces cerevisiae* pheromone response pathway. Mol. Biol. Cell **6:**889–909.
60. **Marcus, S., A. Polverino, M. Barr, and M. Wigler.** 1994. Complexes between STE5 and components of the pheromone-responsive mitogen-activated protein kinase module. Proc. Natl. Acad. Sci. USA **91:**7762–7766.
61. **Marshall, C. J.** 1994. Signal transduction: hot lips and phosphorylation of protein kinases. Nature (London) **367:**686.
62. **Marshall, C. J.** 1995. Specificity of receptor tyrosine kinase signaling: transient versus sustained extracellular signal-regulated kinase activation. Cell **80:**179–185.
63. **Mayer, B. J., H. Hirai, and R. Sakai.** 1995. Evidence that SH2 domains promote processive phosphorylation by protein tyrosine kinases. Curr. Biol. **5:**296–305.
64. **Morgan, D. O., and H. L. De Bondt.** 1994. Protein kinase regulation: insights from crystal structure analysis. Curr. Opin. Cell Biol. **6:**239–246.
65. **Nakamaye, K. L., and F. Eckstein.** 1986. Inhibition of restriction endonuclease NciI cleavage by phosPhorothioate groups and its application to oligonucleotide-directed mutagenesis. Nucleic Acids Res. **14:**9679–9698.
66. **Neiman, A. M., and I. Herskowitz.** 1994. Reconstitution of a yeast protein kinase cascade in vitro: activation of the yeast MEK homolog STE7 by STE11. Proc. Natl. Acad. Sci. USA **91:**3398–3402.
67. **Pawson, T.** 1995. Protein-tyrosine kinases: getting down to specifics. Nature (London) **373:**477–478.
68. **Pelech, S. L.** 1993. Networking with protein kinases. Curr. Biol. **3:**513–515.
69. **Peter, M., A. Gartner, J. Horecka, G. Ammerer, and I. Hershowitz.** 1993. FAR1 links the signal transduction pathway to the cell cycle machinery in yeast. Cell **73:**747–760.
70. **Peter, M., and I. Herskowitz.** 1994. Direct inhibition of the yeast cyclin-dependent kinase Cdc28-Cln by Far1. Science **265:**1228–1231.
71. **Phizicky, E. M., and S. Fields.** 1995. Protein-protein interactions: methods for detection and analysis. Microbiol. Rev. **59:**94–123.
72. **Printen, J. A., and G. F. Sprague, Jr.** 1994. Protein-protein interactions in the yeast pheromone response pathway: Ste5p interacts with all members of the MAP kinase cascade. Genetics **138:**609–619.
73. **Ramer, S., and R. W. Davis.** 1993. A dominant truncation allele identifies a gene, *STE20*, that encodes a putative protein kinase necessary for mating in *Saccharomyces cerevisiae*. Proc. Natl. Acad. Sci. USA **90:**452–456.
74. **Rao, V. N., and S. P. Reddy.** 1994. *elk*-1 proteins interact with MAP kinases. Oncogene **9:**1855–1860.
75. **Reneke, J. E., K. J. Blumer, W. E. Courchesne, and J. Thorner.** 1988. The carboxy-terminal segment of the yeast alpha-factor receptor is a regulatory domain. Cell **55:**221–234.
76. **Rhodes, N., L. Connell, and B. Errede.** 1990. STE11 is a protein kinase required for cell-type-specific transcription and signal transduction in yeast. Genes Dev. **4:**1862–1874.
77. **Roberts, R. L., and G. R. Fink.** 1994. Elements of a single MAP kinase cascade in *Saccharomyces cerevisiae* mediate two developmental programs in the same cell type: mating and invasive growth. Genes Dev. **8:**2974–2985.
78. **Sambrook, J., E. F. Fritsch, and T. Maniatis.** 1989. Molecular cloning: a laboratory manual, 2nd ed. Cold Spring Harbor Laboratory Press, Cold Spring Harbor, N.Y.
79. **Schultz, J., B. Ferguson, and G. F. Sprague, Jr.** 1995. Signal transduction and growth control in yeast. Curr. Opin. Genet. Dev. **5:**31–37.
80. **Sherman, F., G. R. Fink, and J. B. Hicks.** 1986. Methods in yeast genetics. Cold Spring Harbor Laboratory, Cold Spring Harbor, N.Y.
81. **Sikorski, R. S., and P. Hieter.** 1989. A system of shuttle vectors and yeast host strains designed for efficient manipulation of DNA in *Saccharomyces cerevisiae*. Genetics **122:**19–27.
82. **Simon, M.-N., C. De Virgilio, B. Souza, J. R. Pringle, A. Abo, and S. I. Reed.** 1995. Role for the Rho-family GTPase Cdc42 in yeast mating-pheromone signal pathway. Nature (London) **376:**702–705.

83. **Soler, M., A. Plovins, H. Martín, M. Molina, and C. Nombela.** 1995. Characterization of domains in the yeast MAP kinase Slt2 required for functional activity and *in vivo* interaction with protein kinases Mkk1 and Mkk2. Mol. Microbiol. **17:**833–842.
84. **Song, O.-K., J. W. Dolan, Y.-L. O. Yuan, and S. Fields.** 1991. Pheromone-dependent phosphorylation of the yeast STE12 protein correlates with transcriptional activation. Genes Dev. **5:**741–750.
85. **Songyang, Z., et al.** 1995. Catalytic specificity of protein-tyrosine kinase is critical for selective signalling. Nature (London) **373:**536–539.
86. **Sprague, G. F., Jr.** 1991. Assay of the yeast mating reaction. Methods Enzymol. **194:**77–93.
87. **Sprague, G. F., Jr., and J. Thorner.** 1992. Pheromone response and signal transduction during the mating process of Saccharomyces cerevisiae, p. 657–744. *In* E. W. Jones, J. R. Pringle, and J. R. Broach (ed.), The molecular and cellular biology of the yeast *Saccharomyces*: gene expression. Cold Spring Harbor Laboratory Press, Cold Spring Harbor, N.Y.
88. **Stevenson, B. J., N. Rhodes, B. Errede, and G. F. Sprague, Jr.** 1992. Constitutive mutants of the protein kinase STE11 activate the yeast pheromone response pathway in the absence of the G protein. Genes Dev. **6:**1293–1304.
89. **Taylor, S. S., D. R. Knighton, J. Zheng, L. F. Ten Eyck, and J. M. Sowadski.** 1992. Structural framework for the protein kinase family. Annu. Rev. Cell Biol. **8:**429–462.
90. **Teague, M. A., D. T. Chaleff, and B. Errede.** 1986. Nucleotide sequence of the yeast regulatory gene *STE7* predicts a protein homologous to protein kinases. Proc. Natl. Acad. Sci. USA **83:**7371–7375.
91. **Toda, T., S. Cameron, P. Sass, M. Zoller, and M. Wigler.** 1987. Three different genes in S. cerevisiae encode the catalytic subunits of the cAMP-dependent protein kinase. Cell **50:**277–287.
92. **Tyers, M., and B. Futcher.** 1993. Far1 and Fus3 link the mating pheromone signal transduction pathway to three G_1-phase Cdc28 kinase complexes. Mol. Cell. Biol. **13:**5659–5669.
93. **Van Aelst, L. M., S. Barr, S. Marcus, A. Polverino, and M. Wigler.** 1993. Complex formation between RAS and RAF and other protein kinases. Proc. Natl. Acad. Sci. USA **90:**6213–6217.
94. **Whiteway, M., L. Hougan, D. Dignard, D. Y. Thomas, L. Bell, G. C. Saari, F. J. Grant, P. O'Hara, and V. L. MacKay.** 1989. The *STE4* and *STE18* genes of yeast encode potential β and γ subunits of the mating factor receptor-coupled G protein. Cell **56:**467–477.
95. **Wu, C., M. Whiteway, D. Y. Thomas, and E. Leberer.** 1995. Molecular characterization of Ste20p, a potential mitogen-activated protein or extracellular signal-regulated kinase kinase (MEK) kinase kinase from Saccharomyces cerevisiae. J. Biol. Chem. **270:**15984–15992.
96. **Yashar, B., K. Irie, J. A. Printen, B. J. Stevenson, G. F. Sprague, Jr., K. Matsumoto, and B. Errede.** 1995. Yeast MEK-dependent signal transduction: response thresholds and parameters affecting fidelity. Mol. Cell. Biol. **15:**6545–6553.
97. **Zhao, Z.-S., T. Leung, E. Manser, and L. Lim.** 1995. Pheromone signaling in *Saccharomyces cerevisiae* requires the small GTP-binding protein Cdc42p and its activator *CDC24*. Mol. Cell. Biol. **15:**5246–5257.
98. **Zheng, C.-F., and K.-L. Guan.** 1993. Properties of MEKs, the kinases that phosphorylate and activate the extracellular signal-regulated kinases. J. Biol. Chem. **268:**23933–23939.
99. **Zhou, Z., A. Gartner, R. Cade, G. Ammerer, and B. Errede.** 1993. Pheromone-induced signal transduction in *Saccharomyces cerevisiae* requires the sequential function of three protein kinases. Mol. Cell. Biol. **13:**2069–2080.